

Detection Strategies for Bioassays
Based on Enzyme-Amplified
Lanthanide Luminescence

Tanja Steinkamp

Members of the committee:

Chairman:	Prof. Dr. Ir. W.P.M. van Swaaij	Univ. Twente
Secretary:	Prof. Dr. Ir. A. Bliet	Univ. Twente
Promotor:	Prof. Dr. U. Karst	Univ. Twente
Members:	Prof. Dr. Ing. D.A.H. Blank	Univ. Twente
	Prof. Dr. C. Gooijer	VU Amsterdam
	Dr. Ir. J. Huskens	Univ. Twente
	Prof. Dr. B. Krebs	Univ. Münster
	Prof. Dr. G. J. Vancso	Univ. Twente
	Dr. M. Wortberg	BASF Aktiengesellschaft

Publisher: PrintPartners Ipskamp, P.O. Box 333, 7500 AH Enschede,
The Netherlands
www.ppi.nl

© T. Steinkamp, Enschede, 2004.

No part of this work may be reproduced by print, photocopy or other means
without the permission in writing from the publisher.

ISBN 90-365-2063-0

**DETECTION STRATEGIES FOR BIOASSAYS
BASED ON ENZYME-AMPLIFIED
LANTHANIDE LUMINESCENCE**

DISSERTATION

to obtain

the doctor's degree at the University of Twente,

on the authority of the rector magnificus,

prof. dr. F.A. van Vught,

on account of the decision of the graduation committee,

to be publicly defended

on Thursday June 24th, 2004 at 15:00

by

Tanja Steinkamp

Born on March 10th, 1976

in Ankum, Germany

The dissertation has been approved by the promotor:

Prof. Dr. Uwe Karst

Für meine Eltern

Contents

Abbreviations	1
1. Introduction and Scope	5
1.1 Introduction and Scope	5
1.2 References	7
2. Detection Strategies for Bioassays Based on Luminescent Lanthanide Complexes and Signal Amplification	9
2.1 Abstract	9
2.2 Introduction	10
2.3 Enzyme-amplified lanthanide luminescence	15
2.4 Luminescent lanthanide complexes in nanoparticles	25
2.5 Conclusions and Future Perspectives	28
2.6 References	29

3.	Enzyme-Amplified Lanthanide Luminescence for the Reaction Monitoring of the Esterase Catalyzed Ester Cleavage of Tripod Ligands	35
3.1	Abstract	35
3.2	Introduction	36
3.3	Experimental Section	39
3.4	Results and Discussion	42
3.5	Conclusions	49
3.6	References	50
4.	Enzyme-Amplified Lanthanide Luminescence System Based on Pyridinedicarboxylic acid	51
4.1	Abstract	51
4.2	Introduction	52
4.3	Experimental Section	53
4.4	Results and Discussion	63
4.5	Conclusions	77
4.6	References	77

5.	Lanthanide-catalyzed hydrolysis of 4,7-diphenyl-1,10-phenanthroline-2,9-dicarboxylic acid esters	79
5.1	Abstract	79
5.2	Introduction	80
5.3	Experimental Section	81
5.4	Results and Discussion	87
5.5	Conclusions	97
5.6	References	98
6.	Concluding Remarks and Future Perspectives	99
	Summary	101
	Samenvatting	103
	Acknowledgement	105
	Curriculum Vitae	107
	List of Publications	109

Abbreviations

aP	alkaline phosphatase
APCI	atmospheric pressure chemical ionization
BCPDA	4,7-bis-chlorosulfophenyl-1,10-phenanthroline-2,9-dicarboxylic acid
Benz	benzyl
BSA	bovine serum albumin
CDL	curved desolvation line
DMSO	dimethylsulfoxide
DNA	deoxyribonucleic acid
DPPDA	4,7-diphenyl-1,10-phenanthroline-2,9-dicarboxylic acid
DPPDAEE	4,7-diphenyl-1,10-phenanthroline-2,9-dicarboxylic acid diethyl ester
DPPDAiPE	4,7-diphenyl-1,10-phenanthroline-2,9-dicarboxylic acid diisopropyl ester
DPPDAME	4,7-diphenyl-1,10-phenanthroline-2,9-dicarboxylic acid dimethyl ester
DPPDAPE	4,7-diphenyl-1,10-phenanthroline-2,9-dicarboxylic acid dipropyl ester
DPPDAPME	4,7-diphenyl-1,10-phenanthroline-2,9-dicarboxylic acid propyl methyl ester
E	extinction
E2	17 β -estradiol

Abbreviations

EALL	enzyme-amplified lanthanide luminescence
EDTA	ethylenediaminetetraacetic acid
ELISA	enzyme-linked immunosorbent assay
ESI	electrospray ionization
Et	ethyl
FIA	flow-injection analysis
FSA	5-fluorosalicylic acid
FSAP	5-fluorosalicylic phosphate
β -Gal	β -galactosidase
GOD	glucose oxidase
HAc	acetic acid
Hex	hexyl
HL ₁	bis(2-pyridylmethyl)(2-acetoxyphenyl)amine
HPLC	high performance liquid chromatography
HRP	horseradish peroxidase
I	intensity
IgG	immunoglobuline- γ
IR	infrared
iPr	isopropyl
ISC	intersystem crossing
K _i	inhibition constant
K _M	Michaelis-Menten constant
LC-MS	liquid chromatography-mass spectrometry
Ln(III)	lanthanide(III)
LOD	limit of detection

LOQ	limit of quantification
Me	methyl
MRM	multiple reaction monitoring
mRNA	messenger ribonucleic acid
MS	mass spectrometry
NMR	nuclear magnetic resonance
PCR	polymerase chain reaction
PDA	1,10-phenanthroline-2,9-dicarboxylic acid
PDCPE	1,10-phenanthroline-2,9-dicarboxylic acid dipropyl ester
PDC	2,6-pyridinedicarboxylic acid
PDCAh	2,6-pyridinedicarboxaldehyde
PDCEE	2,6-pyridinedicarboxylic acid diethyl ester
PDCIPE	2,6-pyridinedicarboxylic acid diisopropyl ester
PDCME	2,6-pyridinedicarboxylic acid dimethyl ester
PDCPE	2,6-pyridinedicarboxylic acid dipropyl ester
Pr	propyl
PSA	prostate specific antigen
RIA	radioimmunoassay
SA	salicylic acid
SIM	selected-ion monitoring
TIC	total ion current
TRF	time-resolved fluorescence
TSH	thyroid-stimulating hormone
u	units
UV	ultraviolet

Abbreviations

vis	visible
V_{\max}	maximum velocity
XOD	xanthine oxidase

Chapter 1

1.1 Introduction and Scope

In the last few years, enzyme assays and immunoassays gained more and more importance as routinely used tools in clinical chemistry. They are employed for the determination of a variety of analytes, which is mainly due to their outstandingly high selectivity caused by the biochemical reaction. In order to preserve these advantages over the complete assay procedure, high-sensitivity detection schemes have to be developed. For this purpose, the use of time-resolved lanthanide luminescence measurements is of significant interest.[1-3]

Two new lanthanide luminescence-based detection schemes are presented and discussed in **chapter 2**. Besides the enzyme-amplified lanthanide luminescence (EALL), which is the major topic of this thesis, the recently introduced application of nanoparticles containing lanthanide chelate complexes is presented as the second promising technique. An overview over existing assays using EALL and nanoparticles containing lanthanide chelate complexes and a discussion about advantages and disadvantages of the respective techniques complete the chapter.

The known assays employing EALL as detection technique mostly comprise a detection scheme introduced by Evangelista et al., which is based on the hydrolysis of a salicylic phosphate. Therefore, they are restricted to the use of

alkaline phosphatase as marker enzyme.[4] The scope of this thesis was to develop other EALL methods that exploit different enzymes in order to widen the range of applicability of this detection technique. Furthermore, the EALL schemes to be developed were designed to overcome one major disadvantage of the techniques: Their application at a basic pH, which requires the use of EDTA as a co-complexing agent in order to avoid lanthanide hydroxide precipitation. The addition of EDTA results in a small background signal, and therefore the possibility to work at physiological pH should help to reduce the limits of detection for EALL to the low levels, which can be achieved theoretically. The results of the investigations in this field are presented in this thesis.

Chapter 3 describes the employment of an EALL detection scheme for the on-line monitoring of an enzyme-catalyzed ester cleavage. The performance of the EALL technique is compared to monitoring the same reaction by means of ESI-MS. The results of both methods showed good agreement, and it can therefore be concluded that both are suitable for the reaction monitoring of enzymatic reactions.

In **chapter 4**, a new EALL system using 2,6-pyridinedicarboxylic acid (PDC) as sensitizer for Eu(III) and Tb(III) is introduced. This EALL method is applied for the determination of esterases as well as for xanthine oxidase. The measurements are performed close to physiological pH, and therefore addition of EDTA is not necessary.

It was discovered that lanthanide(III) ions are good catalysts for the cleavage of the alkyl esters of 1,10-phenanthroline-2,9-dicarboxylic acid and its derivatives in aqueous solution. The results of the investigations on this topic are summarized in **chapter 5**. The high reaction velocity of the ester hydrolysis indicates that the method might have the potential to be used in organic synthesis.

General conclusions and remarks concerning the advantages and drawbacks as well as future perspectives of the approaches presented in the field of EALL are presented in **chapter 6**, which concludes the thesis.

1.2 References

- [1] Gudgin Templeton, E. F.; Wong, H. E.; Evangelista, R. A.; Granger, T.; Pollak, A. *Clin. Chem.* **1991**, 37, 1506-1512
- [2] Gudgin Dickson, E. F.; Pollak, A.; Diamandis, E. P. *J. Photochem. Photobiol. B* **1995**, 27, 3-19
- [3] Meyer, J.; Karst, U. *Analyst* **2001**, 126, 175-178
- [4] Evangelista, R. A.; Pollak, A.; Gudgin Templeton, E. F. *Anal. Biochem.* **1991**, 197, 213-224

Detection Strategies for Bioassays Based on Luminescent Lanthanide Complexes and Signal Amplification*

2.1 Abstract

Two attractive detection strategies for bioassays are reviewed in this chapter. Both approaches use the highly sensitive time-resolved luminescence of lanthanide complexes in combination with a signal amplification scheme for detection. While the enzyme-amplified lanthanide luminescence (EALL) has been established since more than a decade, nanoparticles doped with luminescent lanthanide complexes have been introduced very recently. In the following, the basic properties and major applications of both techniques are presented, and their future perspectives are critically discussed.

*Steinkamp, T.; Karst, U. accepted for publication in *Analytical and Bioanalytical Chemistry*

2.2 Introduction

Enzyme assays and immunoassays are commonly used tools in clinical chemistry and are applied for the analysis of a large number of important analytes.[1, 2] They are characterized by high selectivity and sensitivity. Improvements in the field of bioassays can either be achieved by optimizing the biochemical processes involved or by progress with respect to the detection scheme used. For the latter purpose, time-resolved lanthanide luminescence detection has been recognized as a powerful approach in recent years and has been summarized in several reviews.[3, 4] This examination focuses on a particular aspect in the field of time-resolved lanthanide luminescence detection: The combination with an amplification step thus yielding a gain in selectivity and sensitivity.

The four lanthanide ions Tb(III), Eu(III), Sm(III) and Dy(III) exhibit characteristic emission spectra with narrow line-shaped emission bands in the visible range of the electromagnetic spectrum. However, it is hard to evoke this emission, which is due to the low molar absorptivity of the naked metal ions.[5] To circumvent this problem, the lanthanide ions are complexed to organic ligands possessing energy levels close to those of the metal ions. The principle of the energy transfer is depicted in figure 2.1:

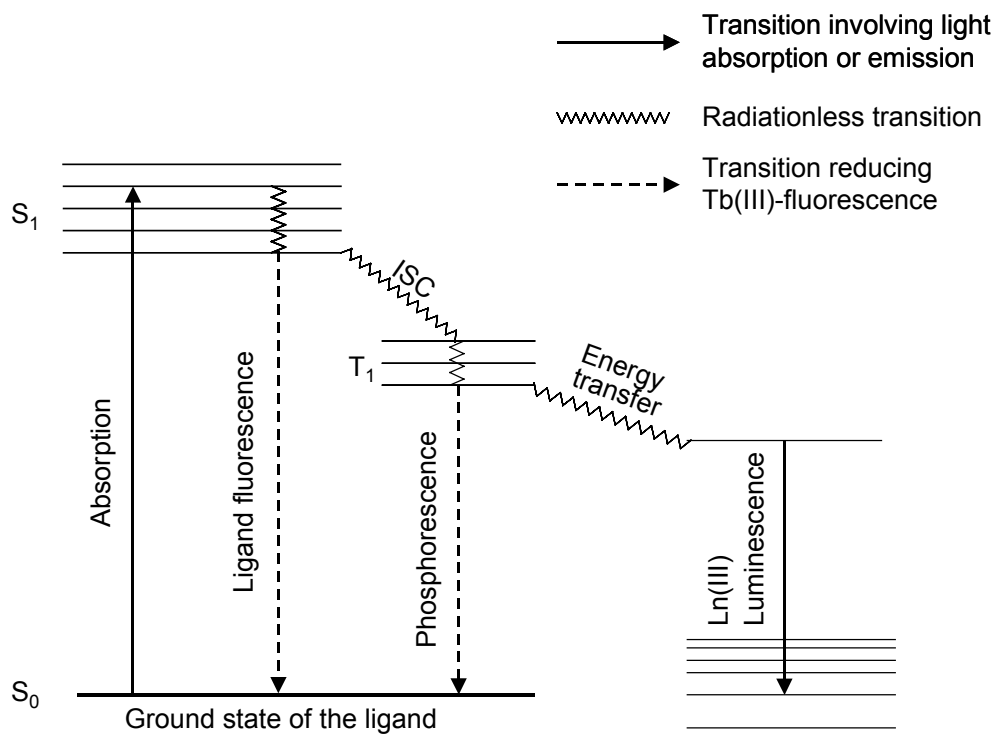


Figure 2.1: Mechanism of the energy transfer from the ligand to the lanthanide(III) ion (ISC = intersystem crossing)

In these complexes, it is possible to excite the ligand by irradiation of light at its excitation wavelength. The absorbed energy is then transferred from the ligand to the central lanthanide ion, which subsequently emits light at its characteristic emission wavelengths.[5] Figure 2.2 shows the emission spectra of Tb(III) and Eu(III) complexes, respectively.

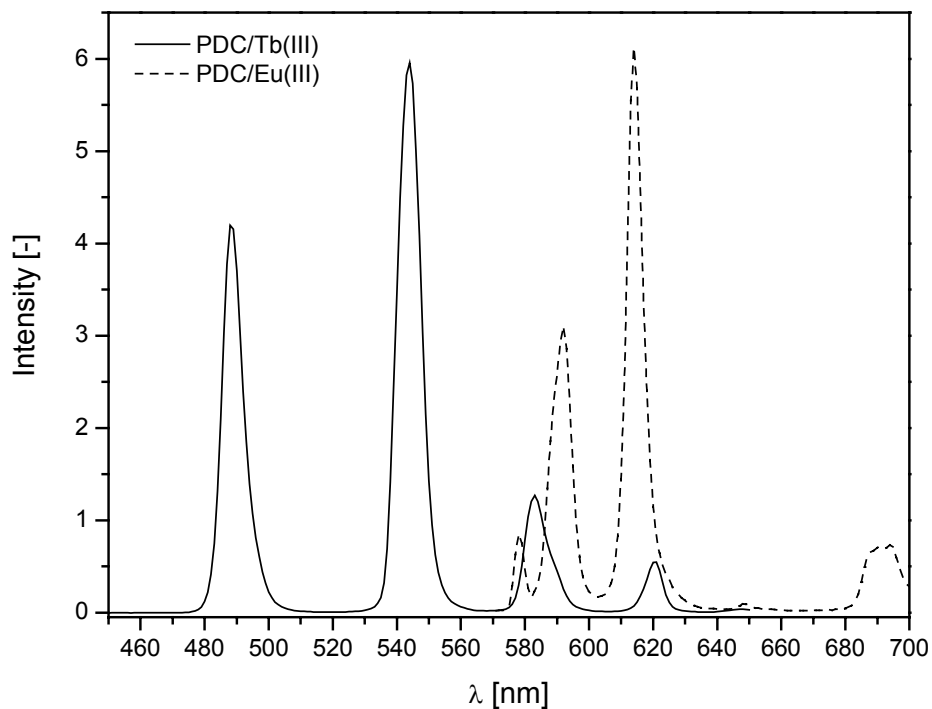


Figure 2.2: Emission spectra of Tb(III) and Eu(III), complexed to 2,6-pyridinedicarboxylic acid (PDC)

The energy transfer accounts for the two great advantages of lanthanide luminescence: First, the extremely large Stokes' shift (often exceeding 200 nm) and second, the long-lived luminescence. Typical decay times of the lanthanide complexes are in the high microsecond or the low millisecond range, thus allowing time-resolved measurements with comparably simple instrumentation. The principle of time-resolved measurements is explained in figure 2.3.

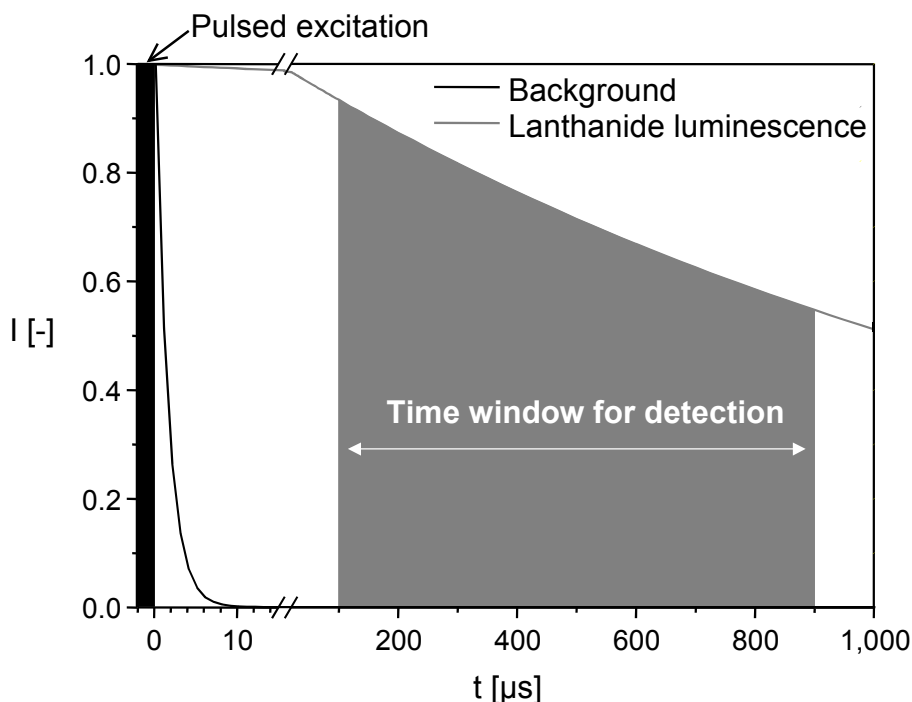


Figure 2.3: *Principle of time-resolved luminescence measurements*

After excitation with a light pulse, mostly from a xenon lamp or a laser, a delay time is used to allow the (almost) complete decay of scattered excitation light and of background fluorescence of organic molecules, typically exhibiting lifetimes in the nanosecond range. Afterwards, the long-lived fluorescence of the lanthanide complexes is selectively recorded.

Based on these properties, lanthanide luminescence has evolved to become a highly sensitive and selective detection method. Lanthanide chelates have become popular labels for immunoassays,[6, 7] and attractive detection schemes have been developed and commercialized, e.g., the Delfia[®] [8] or the FIAgen[™] [9] techniques. However, a further improvement of sensitivity of these methods would allow the detection of even lower analyte

concentrations. Therefore, the combination of amplification strategies with lanthanide luminescence is a highly promising approach.

In recent years, two attractive techniques for the combination of lanthanide luminescence measurements with a coupled amplification step have become available. The first comprises the enzyme-catalyzed formation of a ligand, which is, in contrast to the substrate, able to transfer energy to a lanthanide cation. This strategy combines the enzymatic amplification of established enzyme-linked immunosorbent assays (ELISA) with the sensitivity of lanthanide luminescence techniques and is known as enzyme-amplified lanthanide luminescence (EALL). The second uses luminescent lanthanide complexes that are entrapped in nanoparticles. If the nanoparticles are used as labels in immunoassays, every single particle comprises the luminescent properties of a large number of individual lanthanide complexes. Although both strategies were developed to fulfill similar requirements, they differ significantly with respect to possible applications. The EALL technique is not only capable of detecting affinity reactions with bound enzyme labels, e.g., antibody-antigen or biotin-streptavidin binding, but also enzymatic conversions themselves. Luminescent nanoparticles, however, cannot change their fluorescent properties upon an enzymatic reaction, thus being limited to the detection of affinity assays. On the other hand, the detection scheme for affinity assays using nanoparticles is simpler and can be easier transferred to related applications.

Within this chapter, the most prominent features and applications of both techniques are introduced and critically discussed with particular emphasis on possible future trends. Related techniques utilizing other types of nanoparticles, including those based on semiconductor materials ("quantum dots").[10-12] lanthanide-doped solid-state materials [13, 14] or polymers containing ruthenium complexes with long-lived fluorescence [15] are characterized by attractive properties as well, but are not subject to this evaluation.

2.3 Enzyme-Amplified Lanthanide Luminescence

The term enzyme-amplified lanthanide luminescence (EALL) has been introduced by Evangelista et al. in 1991.[16, 17] In a pioneering article, they introduced a new detection scheme for highly sensitive bioanalytical assays. Here, enzymes were either used as a label or as the analyte of interest.

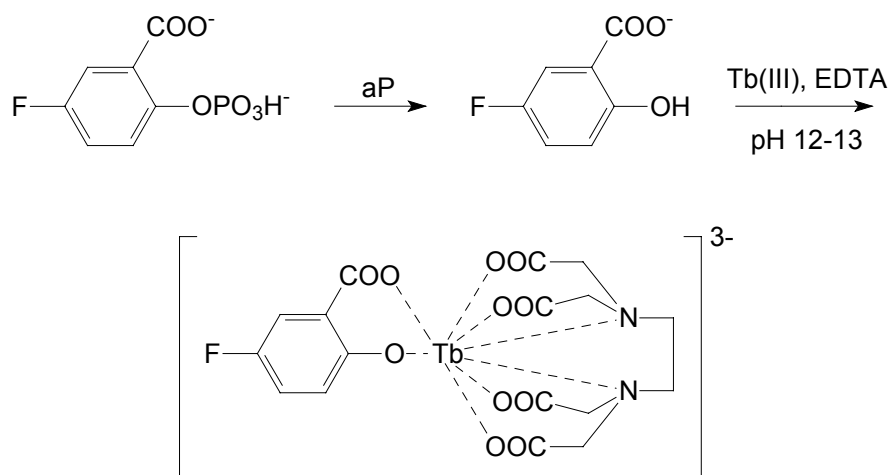


Figure 2.4: Reaction sequence of the aP-catalyzed cleavage of FSAP to FSA with subsequent complexation to Tb(III)/EDTA

A method for the determination of alkaline phosphatase (aP) with the use of 5-fluorosalicylic acid phosphate (FSAP) and Tb(III) was developed (see figure 2.4) and a model immunoassay for rat IgG was performed with alkaline phosphatase as marker. The effectiveness of the EALL principle was demonstrated further by applying the detection scheme for the determination of other hydrolytic and redox enzymes, namely xanthine oxidase (XOD), β -galactosidase (β -Gal) and glucose oxidase (GOD). For xanthine oxidase and β -galactosidase, two other salicylic acid derivatives, salicylaldehyde and salicyl- β -D-galactoside, were employed as substrates for the enzymatic reaction. Both were, after conversion to salicylic acid, complexed to Tb(III). In contrast, for the determination of glucose oxidase 1,10-phenanthroline-2,9-dicarboxylic acid dihydrazide has been used as substrate. In this case, the resulting 1,10-phenanthroline-2,9-dicarboxylic acid forms a luminescent complex with Eu(III). This article already indicated that EALL has the potential to be used as an alternative to enzyme-linked immunosorbent assays (ELISAs) and radioimmunoassays (RIAs).

The same authors used the EALL principle for detection in nucleic acid hybridization assays in microwell, dot-blot and southern blot formats.[18] Regarding the assay, which was performed in microwells, the denatured target DNA sequence (pBR322 linearized with Hind III enzyme) was hybridized with a biotinylated probe (pBR322 BioProbe), and after washing and blocking the unspecific binding sites, aP-labeled avidin was added. For the detection of the aP label, FSAP solution in buffer was given into the well. After incubation, during which the FSAP was cleaved in an aP-catalyzed

reaction to FSA (see figure 4), a solution containing Tb(III) and EDTA was added and the resulting lanthanide luminescence was recorded. In the dot-blot and southern blot assays, which were performed on nylon membranes, 5-*tert*-octylsalicyl phosphate was used as reagent instead of FSAP. In comparison with radioisotopic detection, the authors report a higher sensitivity of the non-isotopic EALL method. In the following, various bio- and immunoassays were developed, which routinely use the EALL principle as detection method. Those assays employ aP as marker and use the cleavage of salicylic phosphate to salicylic acid (SA) with subsequent formation of a luminescent complex with Tb(III) and EDTA. Figure 2.5 illustrates the basic principle of most of those assays.

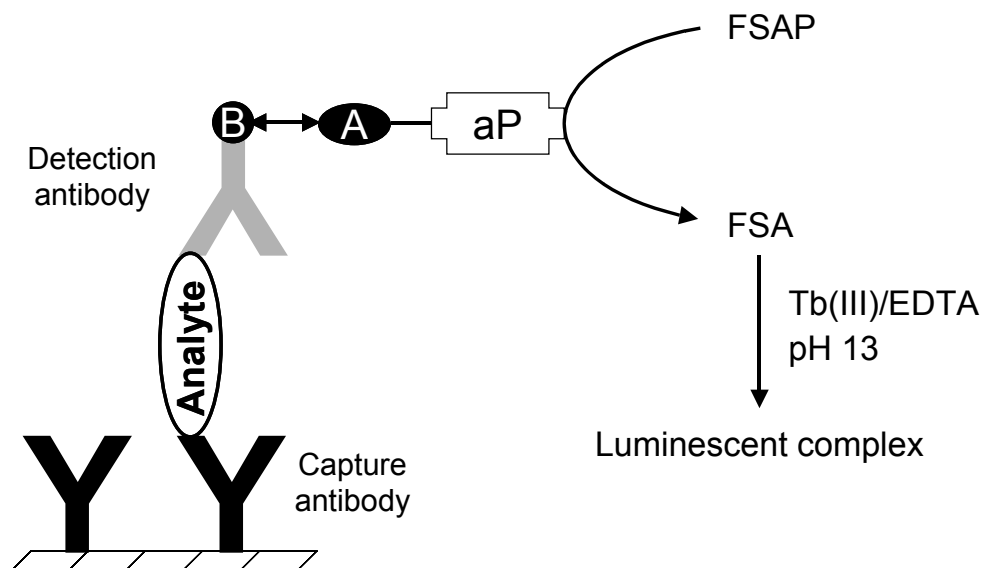


Figure 2.5: Principle of an immunoassay with detection by means of EALL.

The detection antibody is marked with biotin (B), which interacts with aP-labeled avidin (A)

These include the determination of thyrotropin (thyroid-stimulating hormone, TSH) in serum.[19] The samples are pipetted into the wells of a microtiter strip that was previously coated with monoclonal anti-TSH antibody. Biotinylated detection antibody is added, which subsequently reacts with the aP-labeled streptavidin. Detection is performed as described above with FSAP as substrate.

The same assay, and a related one for thyroxine, were used to prove the applicability of 4-methylumbelliferyl phosphate, which was selected of a variety of thirty-three candidate fluorogenic chelators for Eu(III) and Tb(III), as substrate for EALL with Eu(III).[20] In this case, the fluorescence is quenched with ongoing enzymatic reaction because only the phosphate forms luminescent complexes with Eu(III), whereas the generated 4-methylumbelliferone is no sensitizer for lanthanide luminescence.

Later, it was found that phosphotyrosine but not tyrosine itself forms luminescent complexes with Tb(III). Based on this, fluorometric and time-resolved immunofluorometric assays for acidic phosphatase and protein-tyrosine phosphatase activity have been developed.[21]

Some assays for the determination of α -fetoprotein have also been performed using the EALL technique.[22-24] These assays are based, as in case of the thyrotropin assays, on the biotin-streptavidin interactions and aP was again used as label. However, the measurement principles and the employed enzyme substrates evolved in order to enhance the sensitivity. Lianidou and

coworkers for example, used second derivative synchronous scanning fluorescence spectrometry for the screening of a variety of fourteen different bidentate ligands, some of which are compounds of pharmaceutical interest. The most promising, diflunisal (2',4'-difluoro-4-hydroxy-3-biphenylcarboxylic acid), has been converted to its phosphate ester which has been found useful in the EALL-type immunoassay for α -fetoprotein. The same group introduced a sandwich-type immunoassay for interleukin 6, a cytokine that has been implicated in the pathology of several diseases, using diflunisal phosphate as enzyme substrate for aP.[25] In another paper, they described the determination of tumor necrosis factor- α ,[26] a potent pre-inflammatory and immunoregulatory cytokine, which is produced by a large number of different cell types in response to bacterial toxins and inflammatory and other invasive stimuli. Therefore, it is a critical mediator for the diagnosis of a wide variety of diseases.

Another approach has been chosen for the determination of chronic myelogenous leukemia-specific mRNA sequences, also named the Philadelphia translocation. This DNA abnormality can be directly associated with malignancy. Here, the analyte is additionally amplified by a polymerase chain reaction (PCR), after labeling of the PCR primers with biotin or a hapten.[27-30] The immunoassay technique is analogous to the previously mentioned assays, and detection is performed with the FSA/Tb(III)/EDTA-system, too. Similar attempts have been made for the determination of prostate-specific antigen mRNA.[31, 32] Improved quantification of the PCR products was achieved using an internal standard procedure.[33] As template,

a 308 base pair DNA fragment was used, and an internal standard of identical size and identical primers, but with a different centrally located sequence of 26 base pairs was synthesized. As the target analyte is co-amplified with a known amount of the internal standard, the latter compensates for the varying efficiency of the amplification. Again, the FSA/Tb(III)/EDTA system is used for the final detection after hybridization with digoxigenin-modified probes and attachment of an anti-digoxigenin-aP conjugate. The same group later published a similar approach for sandwich-type DNA hybridization assays.[34] A related two-cycle amplification scheme led to a 30-fold improvement of the signal and a ten-fold improvement of the signal-to-noise ratio compared with a single cycle of amplification.[35] However, the repeatability for the two-round amplification scheme is only moderate with relative standard deviations of clearly over 10%.

Barrios and Craik recently used the FSA/Tb(III)/EDTA system to assay the substrate specificity of proteases.[36] In a library of tetrapeptides, FSA was bound to the N-terminus of each peptide. Upon cleavage of the respective amide bond by a protease (compare to figure 2.6), FSA is released and detected as described above. In principle, this approach should also allow a rapid quantitative analysis of other proteases based on dedicated FSA-modified substrates.

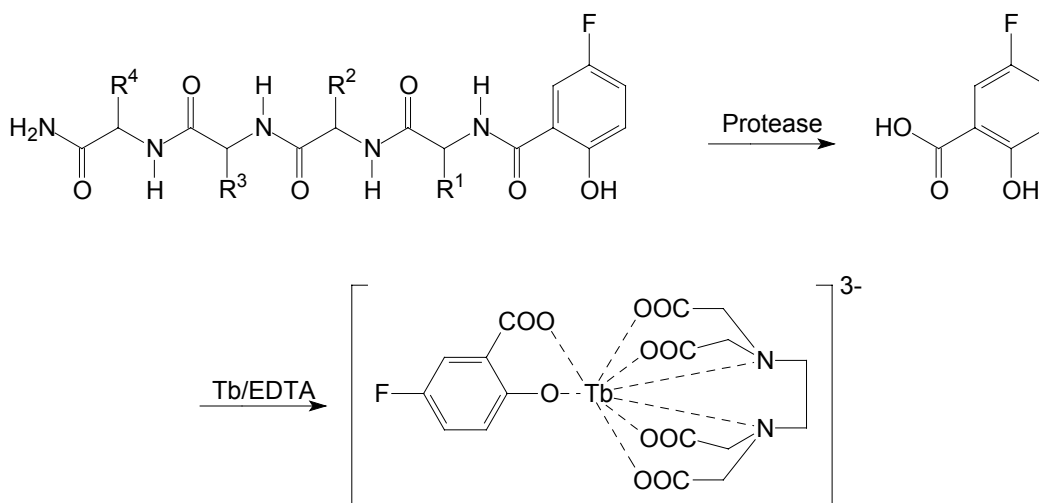


Figure 2.6: Reaction sequence employing the FSA/Tb(III)/EDTA system to evaluate the substrate specificity of proteases (R^1 - R^4 = rest of the respective amino acids)

Other groups made attempts to further increase the number of applications for EALL by using different enzymes and substrates. Xu et al. described an EALL method that uses p-hydroxybenzoic acid as substrate for horseradish peroxidase (HRP) with subsequent detection by means of Tb(III) luminescence.[37] The method has been used for the determination of tuberculosis antibodies. The same group used p-hydroxybenzoic acid to study hemin catalysis.[38] Hemin is often used as substitute for HRP and in this case, it catalyzes the dimerization of p-hydroxybenzoic acid, p-hydroxyphenylacetic acid and p-hydroxyphenylpropionic acid in the presence of H_2O_2 . The reaction scheme is depicted in figure 2.7.

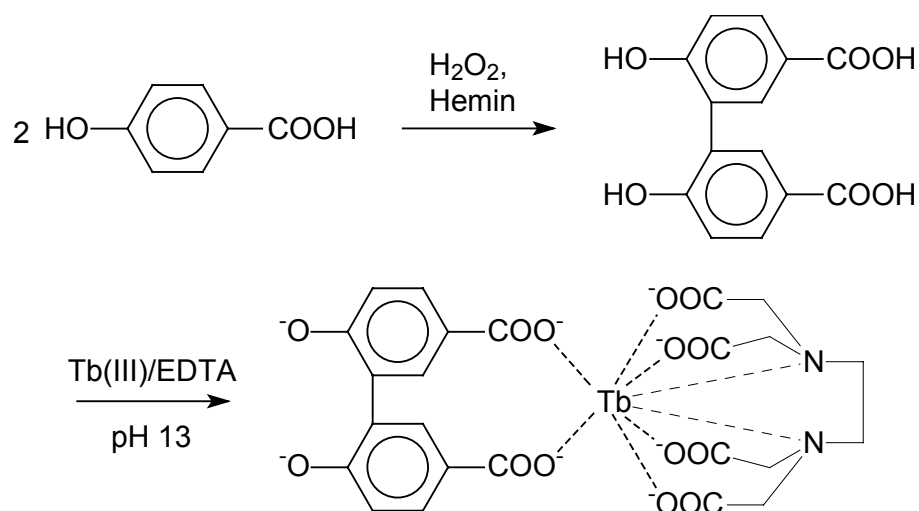


Figure 2.7: Hemin-catalyzed dimerization of p-hydroxybenzoic acid in the presence of H₂O₂; the dimer is subsequently complexed to Tb(III)/EDTA

It was found that only the dimer of p-hydroxybenzoic acid, di-p,p'-hydroxybenzoic acid, forms a luminescent complex with Tb(III), whereas all educts and the dimers of the two other substrates do not sensitize Tb(III). This implies that - in respect of Tb(III) - the complexing site were the two carboxylic acid groups of the dimer of p-hydroxybenzoic acid. Additionally, a simple label assay for a hemin-BSA-conjugate was performed which exhibited a detection limit for the conjugate of $2 \cdot 10^{-10}$ mol/L. In contrast to these results, it was later found that the dimers of a variety of substrates for the reaction described above, in this case catalyzed by HRP, do form luminescent complexes with Tb(III) in the presence of CsCl.[39, 40] Hence, the authors of these articles suggest that the complexation sites for the lanthanide ion are not the carboxylic acid groups but the two hydroxyl groups of the dimer. The limit of

detection for HRP with p-hydroxyphenylpropionic acid as enzyme substrate was in this case $2 \cdot 10^{-12}$ mol/L. This reaction was further applied for the detection of two different ELISAs, one for the determination of goat anti-rabbit IgG, the other for human anti-gliadin IgG in serum. It turned out that detection by means of EALL was applicable for both assays with good results.

Until now, most EALL schemes have been performed at alkaline pH, where the luminescence intensities yield the highest values. However, addition of EDTA at high pH is required in order to avoid precipitation of lanthanide hydroxide. This is very unfavorable for the limits of detection of the EALL methods, because EDTA itself is able to sensitize the lanthanide ions to a minor extent. One of the first EALL methods that can be performed at neutral pH has been developed by Steinkamp et al. after screening a small library of tripod ligands.[41] The ligand bis(2-pyridylmethyl)-(2-hydroxybenzyl)amine (HL₁) has been converted to its acetic acid ester, which was subsequently cleaved in an esterase-catalyzed reaction to the acid (see figure 2.8). Detection was performed by means of Tb(III)-sensitized luminescence.

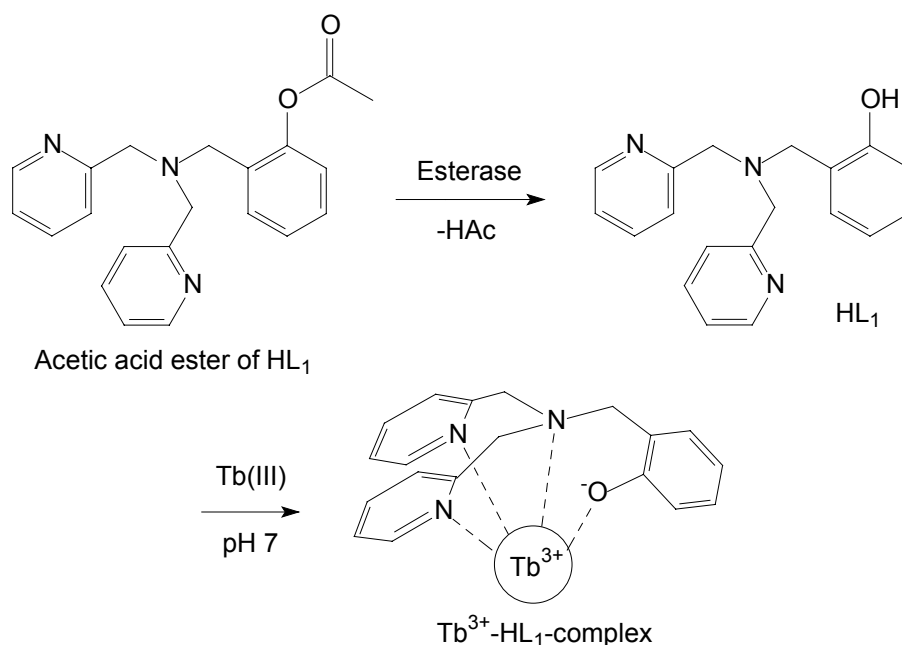


Figure 2.8: Esterase-catalyzed cleavage of HL₁ acetate; the resulting HL₁ is complexed to Tb(III) and the luminescence intensity is read out

Owing to the fact that the tetradentate tripod ligand forms highly stable complexes with Tb(III) and that the luminescence measurements are performed at neutral pH, the addition of co-complexing agents like EDTA can be avoided and background fluorescence is further decreased. With this detection principle, a limit of detection of 10^{-9} mol/L for esterase from porcine liver could be achieved.[41] Based on this reaction, a method for the direct monitoring of an enzymatic conversion has been developed, which was compared to reaction monitoring by means of electrospray ionization mass spectrometry (ESI-MS).[42]

Very recently, another EALL-system that operates at nearly neutral pH without the addition of EDTA has been developed for the determination of esterases or of xanthine oxidase (XOD).[43] It employs 2,6-pyridinedicarboxylic acid (PDC), which is able to sensitize Tb(III) as well as Eu(III) in a very efficient way. PDC has been converted to a variety of alkyl esters, which are then cleaved in an esterase-catalyzed reaction to the diacid again. The reaction scheme is shown in figure 2.9. For the determination of XOD, 2,6-pyridine-dicarboxaldehyde has been used, which also yields PDC when oxidized in the presence of XOD.

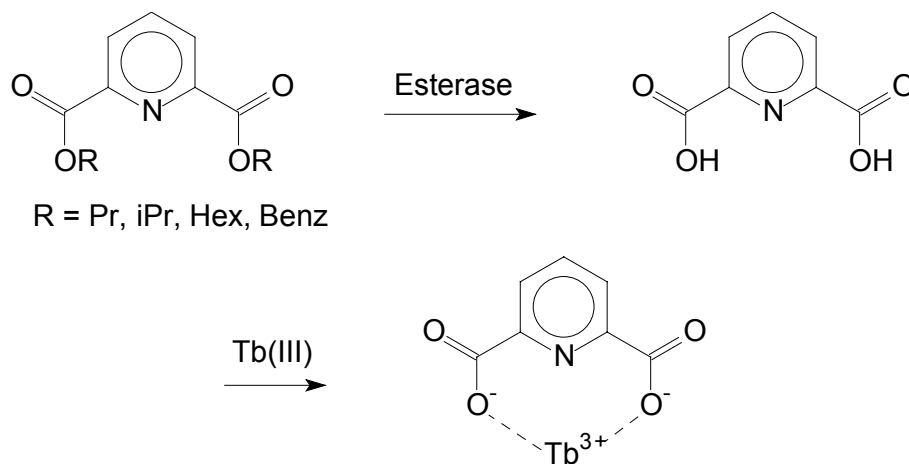


Figure 2.9: Reaction sequence of the esterase-catalyzed hydrolysis of PDC esters with subsequent complexation to Tb(III)

2.4 Luminescent lanthanide complexes in nanoparticles

An attractive approach to enhance the signal intensity of lanthanide luminescence is to enclose a large amount of luminescent lanthanide chelates in one nanoparticle, which is then used as a label in an affinity assay. Until now, the majority of the commercially available nanoparticles contains

Eu(III)/ β -diketonate chelate complexes with a polystyrene cover, exhibiting similar spectroscopic properties than the free chelate complexes in solution.

Härma et al. applied these nanoparticles in different approaches for the determination of prostate specific antigen (PSA).[44-50] A commercially available nanoparticle with an average diameter of 107 nm and tris(naphthyl-trifluorobutanedione) as ligand for Eu(III) is employed. The assay was performed in anti-PSA microplates. Biotinylated PSA was given onto the plate and after incubation and washing, the streptavidin-coated nanoparticle was added. Evaluation was performed by means of TRF imaging after drying of the plate.[44] The principle of the described assay is explained in figure 2.10.

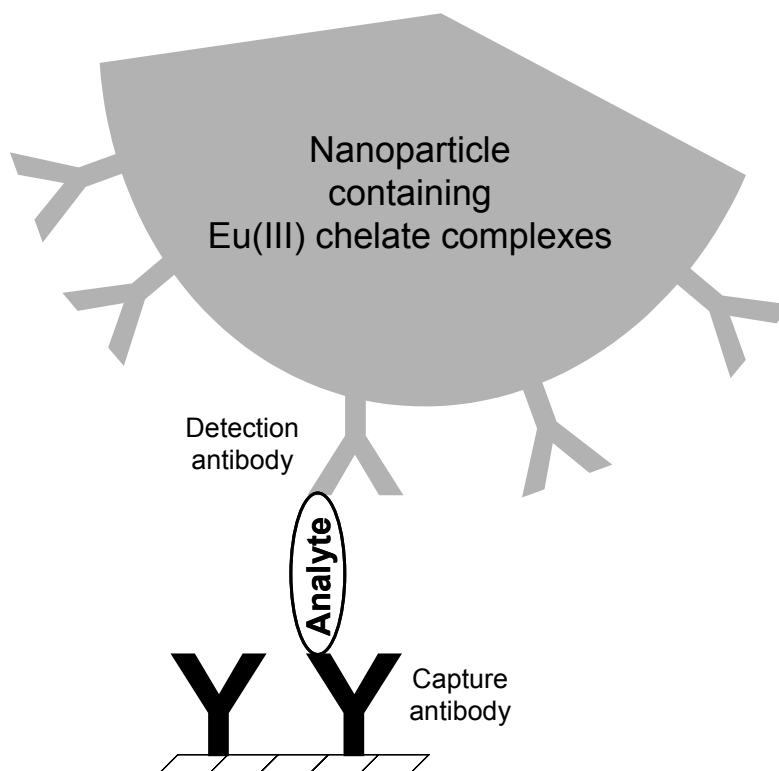


Figure 2.10: Principle of an immunoassay employing nanoparticles containing Eu(III) chelate complexes

The assay was further investigated with respect to solid-phase association and dissociation, non-specific binding and affinity constants of the various binding site density nanoparticle-antibody bioconjugates.[47] Later, the assay could be applied for the determination of real samples, namely PSA in serum.[49] Recently, a paper of these authors described the replacement of the microtitration plate by microparticles with the size of 60-920 μm in diameter.[50]

Eu(III) chelate-dyed nanoparticles with a size of 92 nm have recently been used as donors in a homogeneous proximity-based immunoassay for estradiol.[51] Regarding this competitive assay, the nanoparticles were initially coated with 17 β -estradiol (E2) specific recombinant antibody Fab S16 fragments. The coated particles were given into the bovine serum albumin (BSA)-blocked wells of a microtitration plate. Then, 17 β -estradiol was added which binds to the nanoparticles and after incubation of the plate, an E2-Alexa680-conjugate was pipetted into the wells. AlexaFluor 680 is a near-infrared fluorescent label whose excitation spectrum overlaps with the emission spectrum of Eu(III). Hence, after the E2-Alexa680-conjugate is bound to the remaining free binding sites on the nanoparticle, it is possible to excite the Alexa label with the emission light of the nanoparticle due to the Förster energy transfer taking place between the two luminescent substances.[52] The principle of this assay is depicted in figure 2.11. Detection limits of 70 pmol/L of E2 could be achieved.

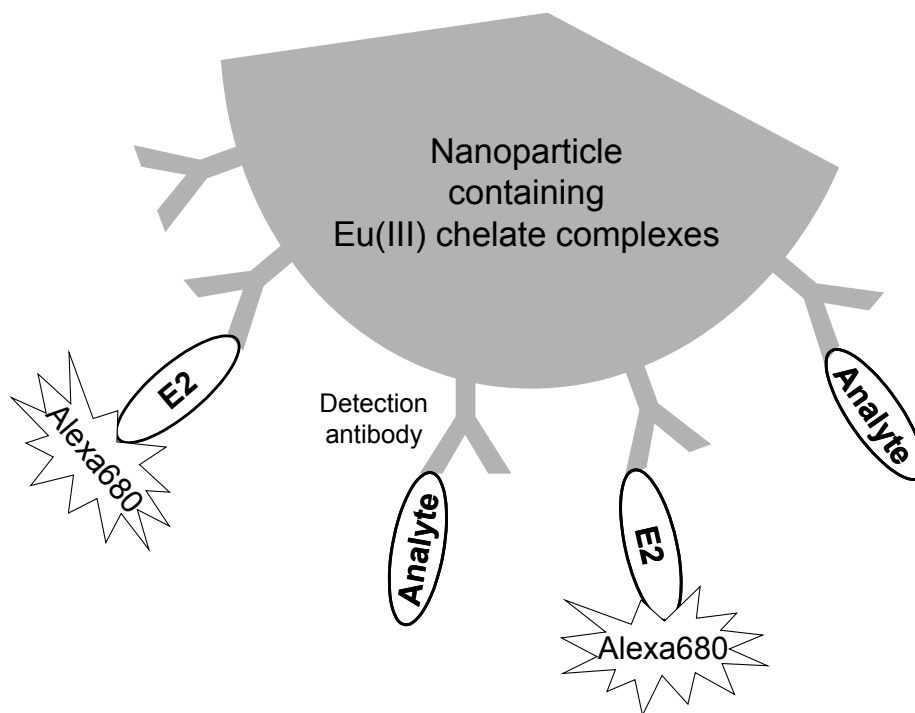


Figure 2.11: Principle of the competitive proximity-based nanoparticle assay for the determination of 17β -estradiol

2.5 Conclusions and Future Perspectives

Despite the attractive properties of both approaches presented in this chapter, they are still used only by a limited number of scientists. With respect to the EALL technique, this is mainly due to the need of laborious development steps to apply the principle to other enzymes than those described in literature. It is not trivial to develop a new EALL system, as the potential substrate must, apart from the required interaction with the enzyme, be characterized by a change from no to a strongly sensitizing effect for one of the four lanthanide cations upon conversion. This certainly hampers the application of EALL for a broader range of enzymes. Furthermore, the EALL

technique requires a slightly higher experimental effort compared with the classical ELISA detection and provides significant advantages only in those cases, where the sensitivity of the detection scheme is the bottleneck for the total sensitivity of a bioassay. On the other hand, there are many situations, in which EALL could solve important analytical problems and certainly would be worth the experimental work. These mainly comprise those cases of enzyme determination, where ultimate sensitivity is required.

In respect of the field of luminescent nanoparticles based on lanthanide chelates, a large expansion may be expected within the next few years. The reason is the possibility to apply this method in a more general way, thus making it easier for industry to provide commercial solutions. The complexity of the detection scheme is lower compared with ELISAs and should allow to at least slightly increase the speed of analysis. Furthermore, multiplexing with at least four different colors should in principle be possible and will add new tools for multianalyte measurements in the future.

For both methods, however, the potential for applications in the field of bioassays is far away from being fully exploited, and new highly selective and sensitive detection schemes based on these approaches certainly can be expected soon.

2.6 References

- [1] Ronald, A.; Stimson, W. H. *Parasitology* **1998**, 117, S13-S27
- [2] Thienpont, L. M.; Van Uytfanghe, K.; De Leenheer, A. P. *Clin. Chim. Acta* **2002**, 323, 73-87
- [3] Lis, S. *Chem. Anal.* **1993**, 38, 443-454
- [4] Georges, J. *Analyst* **1993**, 118, 1481-1486
- [5] Weissman, S. I. *J. Chem. Phys.* **1942**, 10, 214-217
- [6] Hemmilä, I.; Webb, S. *Drug Discovery Today* **1997**, 2, 373-381
- [7] Gudgin Dickson, E. F.; Pollak, A.; Diamandis, E. P. *J. Photochem. Photobio. B* **1995**, 27, 3-19
- [8] Hemmilä, I. *J. Alloys Comp.* **1995**, 225, 480-485
- [9] Evangelista, R. A.; Pollak, A.; Allore, B.; Templeton, E. F.; Morton, R. C.; Diamandis, E. P. *Clin. Biochem.* **1988**, 21, 173-178
- [10] Murphy, C. J.; Coffey, J. L. *Appl. Spec.* **2002**, 56, 16A-27A
- [11] Willard, D. M. *Anal. Bioanal. Chem.* **2003**, 376, 284-286
- [12] Chan, W. C. W.; Nie, S. *Science* **1998**, 281, 2016-2018
- [13] Ji, X. L.; Li, B.; Jiang, S.; Dong, D.; Zhang, H. J.; Jing, X. B.; Jiang, B. *Z. J. Non-Cryst. Solids* **2000**, 275, 52-58
- [14] Bian, L.-J.; Xi, H.-A.; Qian, X.-F.; Yin, J.; Zhu, Z.-K.; Lu, Q.-H. *Mater. Res. Bull.* **2002**, 37, 2293-2301
- [15] Kurner, J. M.; Wolfbeis, O. S.; Klimant, I. *Anal. Chem.* **2002**, 74, 2151-2156
- [16] Evangelista, R. A.; Pollak, A.; Gudgin Templeton, E. F. *Anal. Biochem.* **1991**, 197, 213-224

- [17] Evangelista, R. A.; Gudgin Templeton, E. F.; Pollak, A. *United States Patent* **1993**, No. 5,262,299
- [18] Gudgin Templeton, E. F.; Wong, H. E.; Evangelista, R. A.; Granger, T.; Pollak, A. *Clin. Chem.* **1991**, 37, 1506-1512
- [19] Papanastasiou-Diamandi, A.; Christopoulos, T. K.; Diamandis, E. P. *Clin. Chem.* **1992**, 38, 545-548
- [20] Diamandis, E. P. *Analyst* **1992**, 117, 1879-1884
- [21] Galvan, B.; Christopoulos, T. K. *Clin. Biochem.* **1996**, 29, 125-131
- [22] Christopoulos, T. K.; Diamandis, E. P. *Anal. Chem.* **1992**, 64, 342-346
- [23] Lianidou, E. S.; Ioannou, P. C.; Sacharidou, E. *Anal. Chim. Acta* **1994**, 290, 159-165
- [24] Veiopoulou, C. J.; Lianidou, E. S.; Ioannou, P. C.; Efstathiou, C. E. *Anal. Chim. Acta* **1996**, 335, 177-184
- [25] Bathrellos, L. M.; Lianidou, E. S.; Ioannou, P. C. *Clin. Chem.* **1998**, 44, 1351-1353
- [26] Petrovas, C.; Daskas, S. M.; Lianidou, E. S. *Clin. Biochem.* **1999**, 32, 241-247
- [27] Bortolin, S.; Christopoulos, T. K. *Anal. Chem.* **1994**, 66, 4302-4307
- [28] Bortolin, S.; Christopoulos, T. K. *Clin. Chem.* **1995**, 41, 693-699
- [29] Radovich, P.; Bortolin, S.; Christopoulos, T. K. *Anal. Chem.* **1995**, 67, 2644-2649
- [30] Bortolin, S.; Christopoulos, T. K. *Clin. Biochem.* **1996**, 29, 179-182
- [31] Bortolin, S.; Christopoulos, T. K.; Diamandis, E. P. *Clin. Chem.* **1995**, 41, 1705-1709
- [32] Bortolin, S.; Christopoulos, T. K. *Clin. Biochem.* **1997**, 30, 391-397

- [33] Bortolin, S.; Christopoulos, T. K.; Verhaegen, M. *Anal. Chem.* **1996**, 68, 834-840
- [34] Chiu, N. H. L.; Christopoulos, T. K.; Peltier, J. *Analyst* **1998**, 123, 1315-1319
- [35] Ioannou, P. C.; Christopoulos, T. K. *Anal. Chem.* **1998**, 70, 698-702
- [36] Barrios, A. M.; Craik, C. S. *Bioorg. Med. Chem. Lett.* **2002**, 12, 3619-3623
- [37] Xie, J.-W.; Yan, Y.; Peng, X.-J.; Xu, J.-G.; Chen, G.-Z. *Chem. Abstr.* **1994**, 122:285142
- [38] Zheng, X.-Y.; Lu, J.-Z.; Zhu, Q.-Z.; Xu, J.-G.; Li, Q.-G. *Analyst* **1997**, 122, 455-458
- [39] Meyer, J.; Karst, U. *Analyst* **2000**, 125, 1537-1538
- [40] Meyer, J.; Karst, U. *Analyst* **2001**, 126, 175-178
- [41] Steinkamp, T.; Schweppe, F.; Krebs, B.; Karst, U. *Analyst* **2003**, 128, 29-31
- [42] Steinkamp, T.; Liesener, A.; Karst, U. *Anal. Bioanal. Chem.* **2004**, 378, 1124-1128
- [43] Steinkamp, T.; Karst, U. submitted to *Anal. Chem.*
- [44] Väisänen, V.; Härmä, H.; Lilja, H.; Bjartell, A. *Luminescence* **2000**, 15, 389-397
- [45] Härmä, H.; Soukka, T.; Lönnberg, S.; Paukkunen, J.; Tarkkinen, P.; Lövgren, T. *Luminescence* **2000**, 15, 351-355
- [46] Härmä, H.; Soukka, T.; Lövgren, T. *Clin. Chem.* **2001**, 47, 561-568
- [47] Soukka, T.; Härmä, H.; Paukkunen, J.; Lövgren, T. *Anal. Chem.* **2001**, 73, 2254-2260

- [48] Soukka, T.; Paukkunen, J.; Härmä, H.; Lönnberg, S.; Lindroos, H.; Lövgren, T. *Clin. Chem.* **2001**, 47, 1269-1278
- [49] Soukka, T.; Antonen, K.; Härmä, H.; Pelkkikangas, A.-M.; Huhtinen, P.; Lövgren, T. *Clin. Chim. Acta* **2003**, 328, 45-58
- [50] Härmä, H.; Pelkkikangas, A.-M.; Soukka, T.; Huhtinen, P.; Huopalahti, S.; Lövgren, T. *Anal. Chim. Acta* **2003**, 482, 157-164
- [51] Kokko, L.; Sandberg, K.; Lövgren, T.; Soukka, T. *Anal. Chim. Acta* **2004**, 503, 155-162
- [52] Hemmilä, I.; Mukkala, V.-M. *Crit. Rev. Clin. Lab. Sci.* **2001**, 38, 441-519

Enzyme-Amplified Lanthanide Luminescence for the Reaction Monitoring of the Esterase-Catalyzed Ester Cleavage of Tripod Ligands*

3.1 Abstract

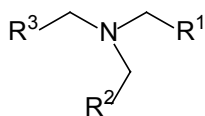
Two complementary methods for reaction monitoring of the esterase-catalyzed cleavage of bis(2-pyridylmethyl)(2-acetoxyphenyl)amine (HL₁) were developed and compared. While enzyme-amplified lanthanide luminescence (EALL) allows for the time-resolved fluorescence determination of the intrinsically non-fluorescent product, both substrate and product of the enzymatic reaction may be determined simultaneously by electrospray ionization mass spectrometry (ESI-MS). Excitation wavelength for the Tb(III) complex of the reaction product is 297 nm and emission was detected at 545 nm, which is the characteristic emission wavelength of the Tb(III) ion. For the mass spectrometric measurements the mass traces were set to $m/z = 306, 328, 348$ and 370 for the protonated ester, the resulting phenol and their sodium adducts, respectively.

*Steinkamp, T.; Liesener, A.; Karst, U. *Anal. Bioanal. Chem.* **2004**, 378, 1124-1128

3.2 Introduction

Screening of a small library of tripod ligands (see table 3.1) resulted in the discovery of bis(2-pyridylmethyl)-(2-hydroxybenzyl)amine (HL₁) as a new sensitizer, which is able to transfer its excitation energy to terbium(III).[1]

Table 3.1: Structures of the screened tripod ligands



Skeletal ligand structure:

Ligand	R ¹	R ²	R ³
HL ₁	2-Hydroxyphenyl	2-Pyridyl	2-Pyridyl
HL ₂	2-Hydroxy-3-tert-butylphenyl	2-Pyridyl	2-Pyridyl
HL ₃	2-Hydroxy-5-nitrophenyl	2-Pyridyl	2-Pyridyl
HL ₄	2-Hydroxyphenyl	3-Methyl-2-pyridyl	2-Pyridyl
HL ₅	2-Hydroxy-3-tert-butylphenyl	3-Methyl-2-pyridyl	2-Pyridyl
HL ₆	2-Hydroxy-5-nitrophenyl	3-Methyl-2-pyridyl	2-Pyridyl
H ₂ L ₇	2-Hydroxyphenyl	2-Pyridyl	2-Hydroxyphenyl
H ₂ L ₈	3-Dibromo-6-hydroxyphenyl	2-Pyridyl	2-Hydroxyphenyl
H ₂ L ₉	3-Dibromo-6-hydroxyphenyl	2-Pyridyl	2-Hydroxy-5-nitrophenyl
H ₂ L ₁₀	2-Hydroxy-5-nitrophenyl	2-Pyridyl	2-Hydroxy-5-nitrophenyl
H ₂ L ₁₁	3,5-Dibromo-6-hydroxyphenyl	2-Pyridyl	2-Hydroxy-5-nitrophenyl
H ₂ L ₁₂	2-Hydroxy-3-tert-butylphenyl	2-Pyridyl	2-Hydroxy-3-tert-butylphenyl

After the synthesis of the acetic acid ester of HL₁, a highly selective method for the determination of porcine liver esterase by means of EALL was developed. Enzyme-catalyzed cleavage of the ester, which is non-fluorescent in the presence of Tb(III), resulted in the formation of HL₁ that forms a highly fluorescent complex with Tb(III). After excitation at 297 nm, the characteristic emission of Tb(III) at 545 nm was observed and used to determine the esterase concentration. As highly stable complexes were formed between the tripod ligands and Tb(III), the addition of EDTA became unnecessary, and background fluorescence was further decreased. Limit of detection for porcine liver esterase with this new EALL method was 10⁻⁹ mol/L, and limit of quantification was 3·10⁻⁹ mol/L. A linear calibration range of two decades starting at the limit of quantification could be obtained.

The only possible spectroscopic way to monitor this reaction is by means of lanthanide luminescence, due to the facts that both educt and product are non-fluorescent and exhibit very similar UV/vis spectra. This chapter describes the extension of the EALL-technique from the sole determination of enzyme concentration to the on-line monitoring of the esterase-catalyzed ester hydrolysis. Furthermore, it was decided to compare the obtained EALL-data with an independent method.

For this purpose, electrospray ionization mass spectrometry was selected. Surprisingly, only few papers have been published on the use of mass spectrometric techniques to monitor enzymatic reactions in solution. The application of electrospray ionization MS in the determination of kinetic

parameters was first reported by Henion et al. in 1995 [2], and since then there has been a number of different approaches to the use of this promising technique in enzymology. Douglas et al. and Konermann et al. have studied the pre-steady state kinetics of enzymatic reactions by means of stopped-flow and time-resolved ESI-MS.[3,4] A short review about this topic has been published by Northrop and Simpson.[5] Siuzdak et al. determined the kinetic parameters for glucosidase- and lipase-catalyzed hydrolysis reactions and demonstrated the significant difference in the kinetic behavior of artificial and natural substrates.[6] Toyokuni et al. utilized ESI-MS in the multiple reaction monitoring (MRM) mode coupled to a flow-injection analysis (FIA) system to investigate the reactivity of α -1,3-fucosyltransferase V as well as the enzyme inhibitor kinetics for this system.[7,8] Leary et al. introduced a “normalization factor” for the direct determination of reaction velocities by use of an internal standard. Thus, it was possible to conclude the Michaelis-Menten constant (K_M), the maximum reaction velocity (v_{max}) and the inhibition constant (K_i) values employing an ESI-ion trap MS system without having to determine external calibration curves.[9]

In the work presented here, electrospray ionization quadrupole MS is used in combination with an autosampler and two HPLC pumps, providing for a simple flow-injection analysis system to simultaneously monitor both the increase of the product concentration as well as the decrease of the substrate concentration.

3.3 Experimental Section

Chemicals

Bis(2-pyridylmethyl)(2-hydroxybenzyl)amine was kindly provided by Dr. Florian Schweppe and Prof. Dr. Bernt Krebs (Institute for Inorganic and Analytical Chemistry, University of Münster, Germany). Bis(2-pyridylmethyl)-(2-acetoxyphenyl)amine was synthesized according to literature.[1] Bis tris propane and esterase from porcine liver (E.C. 3.1.1.1) were purchased from Sigma (Deisenhofen, Germany) in the highest purity available. Terbium(III) chloride hexahydrate was from Aldrich (Steinheim, Germany) and dimethylsulfoxide (p.a.) was purchased from Merck (Darmstadt, Germany). Solvents for LC were methanol (gradient grade) and water for liquid chromatography was from Acros (Geel, Belgium).

Instrumentation

All fluorimetric determinations were carried out with the microplate reader model FLUOstar from BMG LabTechnologies (Offenburg, Germany) with FLUOstar software version 2.10-0. Due to the fact that no filter with the exact excitation wavelength of the complex (297 nm) was available, excitation was accomplished at a wavelength of 290 nm (± 15 nm). For emission measurements, a dedicated narrow-bandwidth filter for Tb(III) emission at $\lambda = 545$ nm (± 10 nm) was used. Electrospray ionization-mass spectrometry (ESI-MS) was performed on a Shimadzu LCMS QP8000 single quadrupole mass spectrometer with an electrospray ionization probe coupled to a flow injection system comprising an autosampler (Shimadzu, SIL-10A), a controller unit (Shimadzu, SCL-10Avp) and two HPLC pumps (Shimadzu, LC-10ADvp).

The setup control and data evaluation were performed using the Shimadzu Class 8000 V1.20 software.

Solution preparation

The used esterase (from porcine liver E.C. 3.1.1.1) as well as the terbium(III) chloride solution, the bis tris propane buffer and the acetic acid ester of bis(2-pyridylmethyl)(2-hydroxybenzyl)amine (HL_1) were dissolved in water for liquid chromatography. To ensure sufficient solubility of the ester, 20 % (v/v) dimethylsulfoxide were added to the ester stock solution with a concentration of 10^{-3} mol/L. All further dilution steps were made by addition of water to the stock solution.

Time-resolved fluorescence measurements (on-line)

50 μ L of a 10^{-3} mol/L Tb(III) solution were pipetted into 3×12 wells of a 96 well microplate. Afterwards, 50 μ L of ester solution with the concentrations 10^{-4} mol/L, $6 \cdot 10^{-5}$ mol/L and $3 \cdot 10^{-5}$ mol/L were added into 12 wells each. Then, 50 μ L of bis tris propane buffer solution (pH 7.4, 0.01 mol/L) were added into each well. In the last 4 wells of each row, 50 μ L of water were pipetted for the blank and in the remaining 3×8 wells 50 μ L of esterase solution (1 u/mL) were given. Afterwards, the fluorescence intensity was measured with a delay time of 50 μ s and an integration time of 1 ms. Excitation wavelength was 290 nm and emission wavelength was 545 nm. The fluorescence intensity was determined in intervals of five minutes.

Time-resolved fluorescence measurements (off-line)

For all three concentrations of ester (10^{-4} mol/L, $6 \cdot 10^{-5}$ mol/L and $3 \cdot 10^{-5}$ mol/L) the measuring procedure was as follows: First, 5 mL of ester solution and 5 mL of esterase solution (1 u/mL) were mixed. 100 μ L of this mixture were pipetted immediately into 12 wells of different microplates each. Another row of those plates was filled with 50 μ L of ester solution and 50 μ L water. Every five minutes, 50 μ L of terbium chloride solution and 50 μ L of buffer were added to one of the plates. Subsequent fluorescence measurements of this plate were accomplished in the same way as for the online measurements.

Mass spectrometric analysis

For all three concentrations of ester (10^{-4} mol/L, $6 \cdot 10^{-5}$ mol/L and $3 \cdot 10^{-5}$ mol/L), the mass spectrometric procedure was as follows: 2 mL of esterase solution (1 u/mL) and 2 mL of ester solution were mixed. From this reaction mixture, 1.5 mL were transferred into a HPLC vial. An autosampler injected first after 2.25 minutes reaction time 5 μ L of the uncleansed reacting solution into a solvent stream consisting of methanol/water (50/50, v/v) with a flow rate of 0.2 mL/min. Subsequent injections out of the reaction vial took place every 4 minutes. Thus, the samples were introduced into the ESI-MS. They were analyzed in the positive ion mode using selected-ion monitoring (SIM). The mass traces were set to $m/z = 306, 328, 348$ and 370 for the protonated ester, the resulting phenol and their sodium adducts, respectively. For all measurements, a curved desolvation line (CDL)-voltage of -35 V and a CDL temperature of 230 °C were used. The deflector voltage was 35 V and

the detector voltage was 1.6 kV. The ESI parameters comprised a probe voltage of +3.0 kV and a nebulizer gas flow-rate of 4.5 L/min.

Mass spectrometric data analysis

For evaluation, the different mass traces were extracted and the resulting peaks were integrated. The signals for the protonated species and the corresponding sodium adducts were summed up. Determination of the actual concentration was achieved by external calibration for both substrate (the ester) and resulting product (the phenol).

3.4 Results and Discussion

The esterase-catalyzed hydrolysis of bis(2-pyridylmethyl)(2-acetoxyphenyl)-amine is presented in figure 3.1:

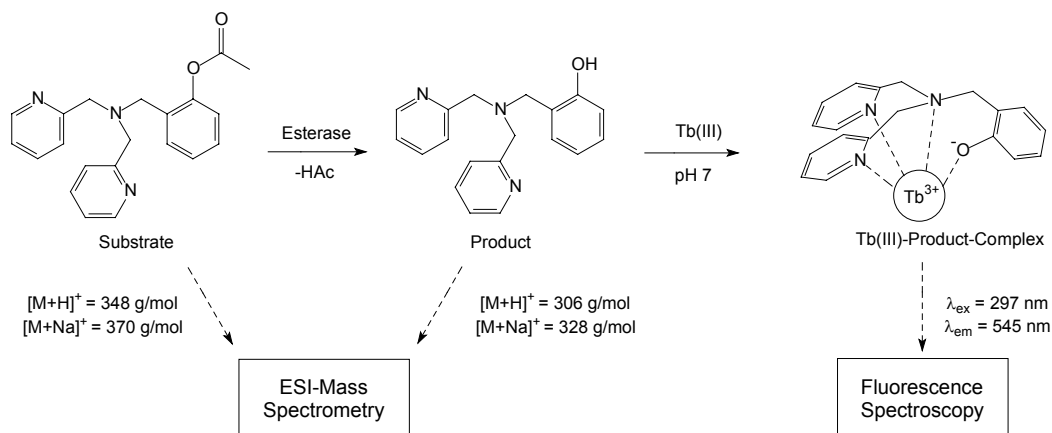


Figure 3.1: Reaction scheme for the enzymatic cleavage of the ester of HL₁ and the complex formation of the product with Tb(III) as well as detection scheme for the fluorescence spectroscopic and ESI-mass spectrometric determination of substrate and product

In contrast to the substrate, the reaction product bis(2-pyridylmethyl)-(2-hydroxybenzyl)amine (HL_1) fulfills both requirements for lanthanide-sensitized luminescence: It forms a complex with Tb(III) and is able to transfer its excitation energy to the central ion, resulting in intense luminescence emission at $\lambda = 545 \text{ nm}$. The fluorescence spectra of the Tb(III)/ HL_1 -complex are depicted in figure 3.2:

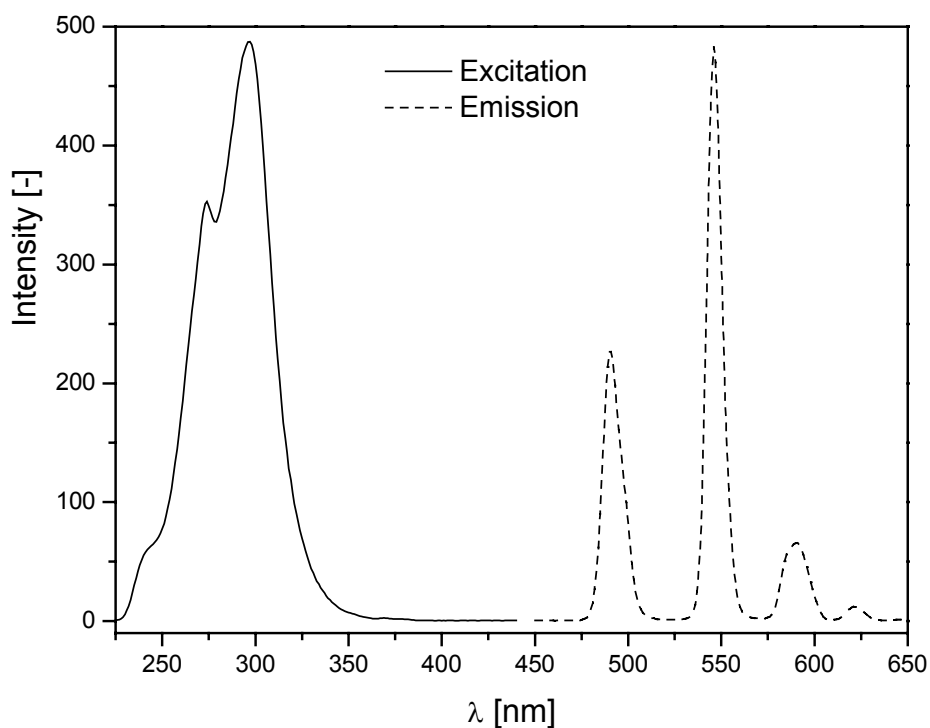


Figure 3.2: Excitation spectrum and emission spectrum of the Tb(III)- HL_1 complex (λ_{em} for Excitation: 545 nm; λ_{ex} for Emission: 297 nm)

The lanthanide luminescence may be detected in the time-resolved mode with a delay time of 50 μs and an integration time of 1 ms. In contrast to other lanthanide luminescence systems, substrate and product molecule are non-fluorescent and exhibit very similar UV/vis absorption spectra. Therefore, both

native fluorescence spectroscopy and UV/vis spectroscopy are not suitable for reaction monitoring of this enzymatic conversion. This is illustrated in figure 3.3, where the UV/vis spectra of approximately 10^{-4} mol/L solutions of substrate and product are presented.

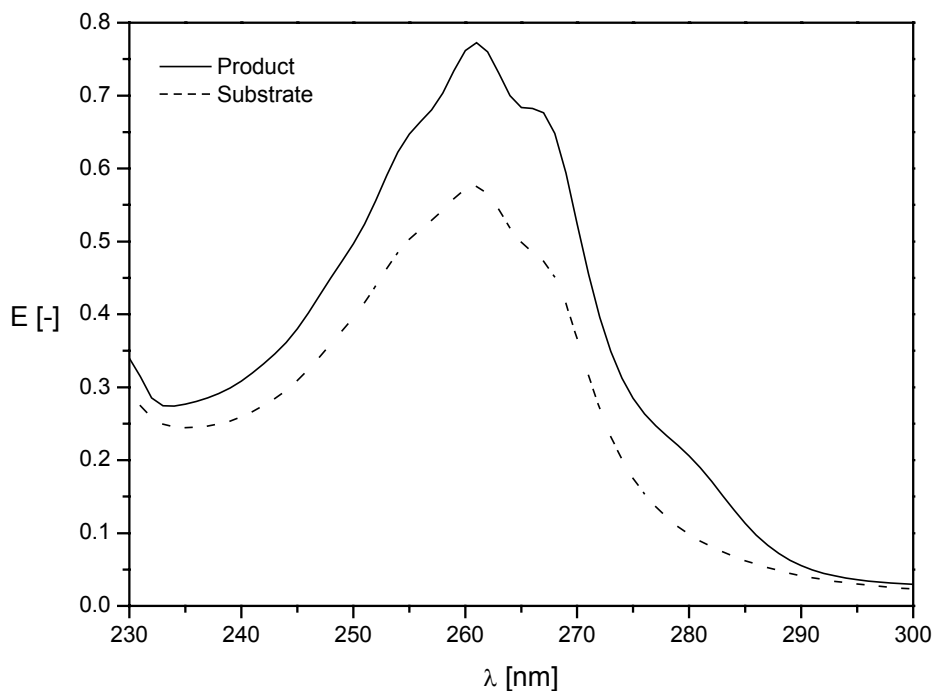


Figure 3.3: UV/vis absorption spectra of substrate (HL_1E) and product (HL_1)

Both exhibit significant absorbance in the wavelength range between 230 nm and 300 nm. However, as the absorbance for both substances can be traced back mostly to the three aromatic rings, and only to a lesser extent to the additional functional groups, the differences between the UV/vis spectra of both substances are so small that they cannot be used to monitor the enzymatic conversion.

Initially, the suitability of this system for on-line monitoring of the enzymatic conversion was investigated. Depending on the substrate concentration, the maximum fluorescence was measured between 10 and 20 minutes. However, the fluorescence intensity decayed rapidly again, and no constant value was obtained. As the same wells of the microplate are irradiated multiply with UV light below 300 nm when using this approach, it is assumed that photobleaching of the substrate and/or product molecules occurs. For this reason, an off-line approach was developed. Here, each well of the microplate is read out only once, reducing the likelihood of photobleaching. For the off-line measurements, a constant fluorescence intensity was observed after 40 minutes for all three substrate concentrations investigated. The respective data is presented in figure 3.4:

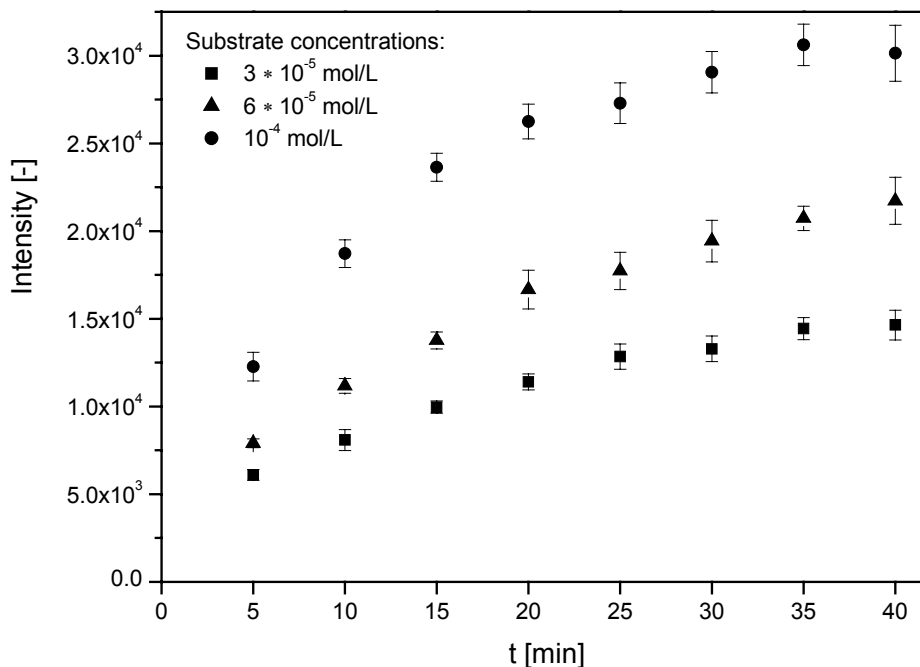


Figure 3.4: Reaction monitoring of the ester cleavage by means of time-resolved fluorescence spectroscopy

Calibration was performed externally using pure standards of substrate and product. The error bars represent the relative standard deviation ($n=8$) for multiple determination of the fluorescence intensity in different wells of one microplate. Under the conditions applied in this work, the limit of detection for the product is 10^{-5} mol/L.

For comparison and validation purposes, a second and independent analytical method was developed. Due to the basic properties of both substrate and product, it was expected that both might be analyzed easily by electrospray ionization mass spectrometry in the positive ion mode. First experiments showed that both substances are detected well as protonated pseudomolecular ions $[M + H]^+$ or as sodium adducts $[M + Na]^+$ in a mass spectrometer after electrospray ionization (ESI) or atmospheric pressure chemical ionization (APCI). As the ESI results were superior to the APCI results, due to a better signal-to-noise ratio, ESI-MS was selected for all further measurements. The substrate was detected at the mass trace of $m/z = 348$ for the protonated substance and at $m/z = 370$ for its sodium adduct. For the product, $m/z = 306$ and $m/z = 328$ were selected to monitor the protonated molecule and the sodium adduct, respectively. The active reaction mixture was injected into the mass spectrometer approximately any four minutes. Although a continuous reaction monitoring by constant infusion of the reaction mixture is in principle possible, the off-line approach was selected to avoid constant infusion of non-volatile matter into the interface, which could result in clogging of the curved desolvation line (CDL). With a modern orthogonal ESI source, these problems should be observed to a lesser extent or not at all.

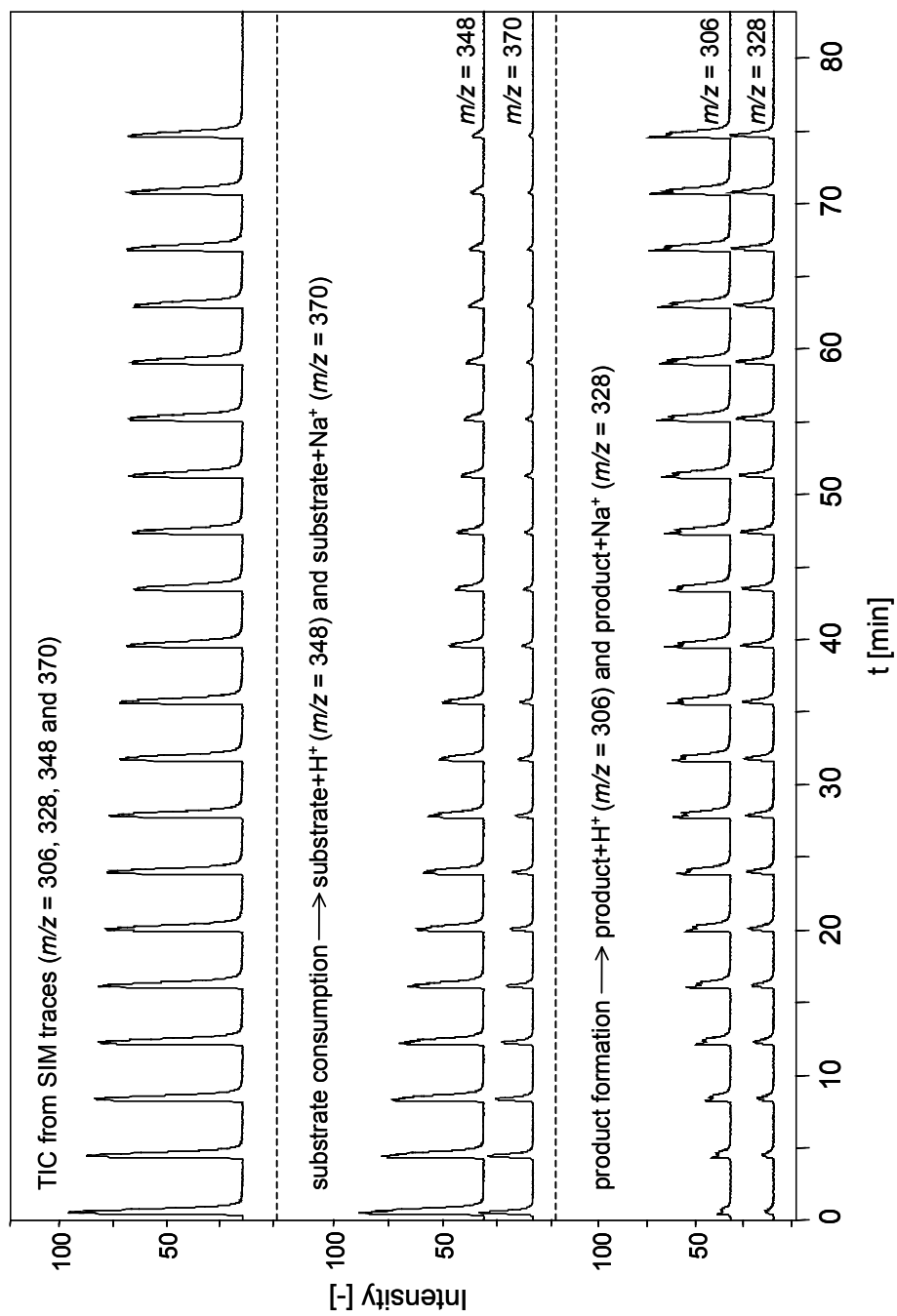


Figure 3.5: Reaction monitoring of the ester cleavage by ESI-MS.

In the upper part of figure 3.5, the total ion current (TIC) of the sum of the selected ion monitoring (SIM) traces of $m/z = 306, 328, 348$ and 370 is presented. As the TIC is decreasing slightly with time, it is obvious that the two ions associated with the substrate are detected with slightly better intensity than the two respective ions of the product. The individual mass traces are presented in the lower parts of figure 3.5.

In figure 3.6, the sum of the intensity of the $[M + H]^+$ and $[M + Na]^+$ peaks for substrate and product is presented depending on the reaction time.

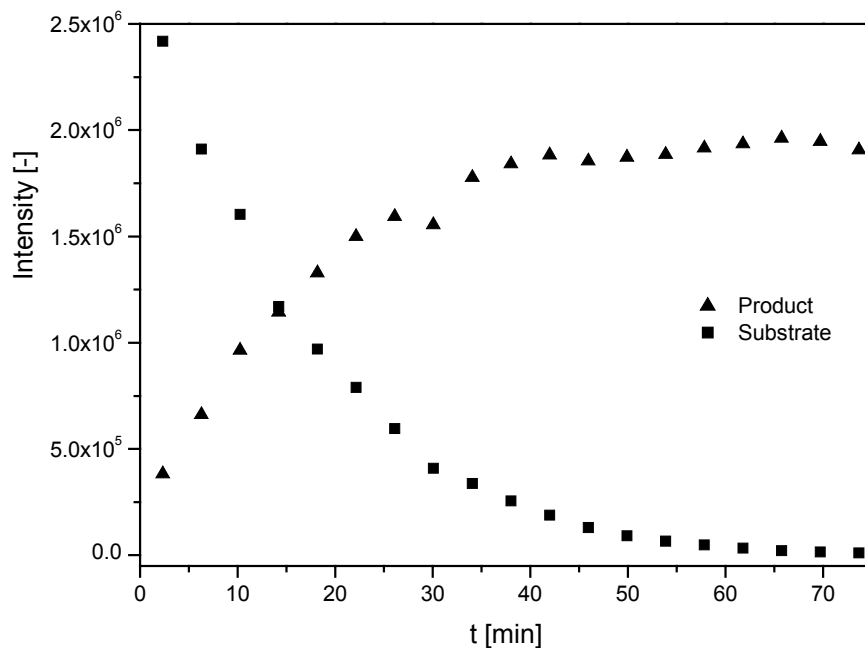


Figure 3.6: Reaction monitoring of the ester cleavage by ESI-MS ($c_{(ester)} = 6 \cdot 10^{-5}$ mol/L). The $[M + H]^+$ and $[M + Na]^+$ peaks have been summed up for substrate and product

It is obvious that, as in case of the fluorescence measurements, a constant value is observed already after 40 minutes for a concentration of $6 \cdot 10^{-5}$ mol/L.

For the other substrate concentrations, the data from time-resolved fluorescence spectroscopy were confirmed as well. Under these conditions, the limits of detection for the substrate and the product are 10^{-5} mol/L, respectively.

3.5 Conclusions

It can be concluded that both enzyme-amplified lanthanide luminescence and electrospray ionization mass spectrometry are useful methods for the monitoring of enzyme-catalyzed ester hydrolysis when using this type of substrates. The two methods complement each other very well: The EALL technique may already be carried out on a simple and cheap standard fluorescence spectrometer, although a time-resolved fluorescence spectrometer with microsecond resolution provides superior results. The ESI-MS method is advantageous in terms of the possibility of monitoring the substrate and product concentrations simultaneously. Therefore, two sets of data points are obtained in one single experiment. Furthermore, the ESI-MS method is, due to its high selectivity, likely to exhibit less interferences in complex matrices. Both detection methods are simple and comparably robust, and good results are obtained already under the optimum conditions for the enzymatic conversion. It is not necessary to change the pH, solvents etc. prior to analysis. Thus, both methods are useful in the easy and routine monitoring of reactions and complement each other in a feasible way. It can therefore be expected that both methods may find increased future use for the monitoring of enzymatic reactions.

3.6 References

- [1] Steinkamp, T.; Liesener, A.; Karst, U. *Anal. Bioanal. Chem.* **2004**, 378, 1124-1128
- [2] Hsieh, F. Y. L.; Tong, X.; Wachs, T.; Ganem, B.; Henion, J. *Anal. Biochem.* **1995**, 229, 20-25
- [3] Zechel, D. L.; Konermann, L.; Withers, S. G.; Douglas, D. J. *Biochemistry* **1998**, 37, 7664-7669
- [4] Kolakowski, B. M.; Simmons, D. A.; Konermann, L. *Rapid Commun. Mass. Spectrom.* **2000**, 14, 772-776
- [5] Northrop, D. B.; Simpson, F. B. *Bioorgan. Med. Chem.* **1997**, 5, 641-644
- [6] Bothner, B.; Chavez, R.; Wei, J.; Strupp, C.; Phung, Q.; Schneemann, A.; Siuzdak, G. *J. Biol. Chem.* **2000**, 275, 13455-13459
- [7] Norris, A. J.; Whitelegge, J. P.; Faull, K. F.; Toyokuni, T. *Biochemistry* **2001**, 40, 3774-3779
- [8] Norris, A. J.; Whitelegge, J. P.; Faull, K. F.; Toyokuni, T. *Anal. Chem.* **2001**, 73, 6024-6029
- [9] Ge, X.; Sirich, T. L.; Beyer, M. K.; Desaire, H.; Leary, J. A. *Anal. Chem.* **2001**, 73, 5078-5082

Enzyme-Amplified Lanthanide Luminescence System Based on Pyridinedicarboxylic Acid*

4.1 Abstract

2,6-Pyridinedicarboxylic acid (PDC) derivatives are introduced as new substrates for enzyme-amplified lanthanide luminescence (EALL). Various PDC esters have been synthesized as esterase substrates that are cleaved to PDC in the presence of the enzyme. PDC forms luminescent complexes with Tb(III) or Eu(III), and the evaluation of the reaction is used for the selective and sensitive detection of esterases. As a second model reaction, xanthine oxidase (XOD) catalyzes the oxidation of 2,6-pyridinedicarboxaldehyde to PDC. Major advantage of the tridentate PDC ligand is the possibility to perform all steps of the assay within or close to the physiological pH range, while the established EALL schemes based on bidentate salicylates or bisphenols have to be carried out at strongly alkaline pH to ensure sufficient complexation with the lanthanides.

*Steinkamp, T.; Karst, U. submitted for publication to *Analytical Chemistry*

4.2 Introduction

The highest fluorescence intensities for lanthanide salicylate complexes, which are the most commonly used EALL substrates, are obtained at alkaline pH values, because the involved salicylates and phenols have to be deprotonated to ensure sufficient complexation with the central cations.[1-3] On the other hand, the lanthanide ions tend to precipitate as insoluble hydroxides at alkaline pH. For this reason, additional co-ligands such as EDTA are used to keep the lanthanides in solution. Unfortunately, these co-ligands are able to transfer an extremely small, but still measurable amount of energy to the central ions, thus resulting in a limitation of sensitivity of the method by the blank.[4] To overcome this problem, it is important to find ligands, which are able to form complexes and to transfer excitation energy under conditions close to the physiological pH.

Therefore, a new sensitizer system should be developed under consideration of the following criteria: Most importantly, the involved enzymatic reaction should result in the formation of a carboxylate-functionalized sensitizer to allow application to many different enzyme systems (esterases, xanthine oxidase, proteases, etc.). Furthermore, operation of the reaction at neutral pH without addition of further complexing agents should be possible. Therefore, a series of literature-known sensitizers for lanthanides with carboxylate functions was considered. Finally, 2,6-pyridinedicarboxylic acid (PDC) was selected due to its strong complexation abilities (tridentate ligand) and due to the fact that it is known to be a sensitizer not only for Tb(III), but also for Eu(III).[5] The respective investigations are described in this chapter.

4.3 Experimental Section

Chemicals

All chemicals were purchased from Aldrich (Steinheim, Germany) in the highest purity available, except the following substances: Bis tris propane (1,3-bis[tris(hydroxymethyl)methylamino]propane) and xanthine oxidase from microorganisms were purchased from Sigma (Deisenhofen, Germany) in the highest purity available. Esterase from hog liver (E.C. 3.1.1.1), esterase from bacillus stearothermophilus (E.C. 3.1.1.1), esterase from Bacillus sp. (E.C. 3.1.1.1) and pyridine were obtained from Fluka (Neu-Ulm, Germany). 2-propanol and DMSO were purchased from Merck (Darmstadt, Germany), diethyl-2,6-pyridinedicarboxylate and 2,6-pyridinedicarboxaldehyde from TCI (Zwijndrecht, Belgium), europium trichloride hexahydrate from Acros (Geel, Belgium) and cesium chloride from AppliChem (Darmstadt, Germany).

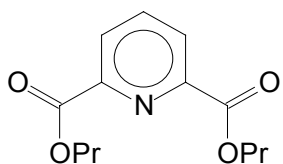
Instrumentation

All quantitative determinations were carried out using a microplate reader from BMG LabTechnologies (Offenburg, Germany) with FLUOstar software version 2.10-0. The used excitation filter had a wavelength of 280 ± 10 nm, and the respective emission filters were characterized by wavelengths of 545 ± 10 nm (for Tb(III)), 570 ± 10 nm (for Dy(III)), 615 ± 10 nm (for Eu(III)) and 640 ± 10 nm (for Sm(III)). The fluorescence spectra were recorded using a fluorescence spectrometer AMINCO-Bowman series 2 from Polytec GmbH (Waldbronn, Germany) with AB 2 software version 5.00. For all measurements, a spectral bandwidth of 4 nm was applied.

Synthesis of dipropyl-2,6-pyridinedicarboxylate, diisopropyl-2,6-pyridinedicarboxylate, dihexyl-2,6-pyridinedicarboxylate and dibenzyl-2,6-pyridinedicarboxylate

To an ice-cooled mixture of 4.9 mmol of the dry alcohol in 3 mL of dry pyridine, 2.45 mmol (0.5 g) of 2,6-pyridinedicarboxyl dichloride were added dropwise under stirring. The mixture was then allowed to stir over night at room temperature. Subsequently, it was poured onto ice water, and hydrochloric acid was carefully added until the pH was slightly acidic. The precipitate was washed with NaHCO₃ solution, filtered off and dried. In case of dipropyl-2,6-pyridine dicarboxylate, the ester did not precipitate. The solvent was therefore removed by means of vacuum evaporation, and a yellowish viscous liquid was obtained.

The esters were characterized by means of elemental analysis, ¹H-NMR, ¹³C-NMR, mass spectrometry and infrared spectroscopy as described in the following:



Dipropyl-2,6-pyridinedicarboxylate (PDCPE):

Elemental analysis: C: 62.07% (calc.: 62.14%); H: 6.48% (calc.: 6.82%);
N: 5.82% (calc.: 5.57%)

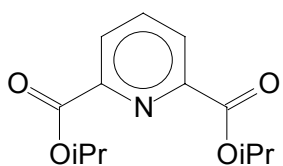
¹H-NMR (300 MHz, CDCl₃): δ [ppm] = 8.25 (d, 2H, py-H); 8.0 (t, 1H, py-H); 4.4 (t, 4H, -O-CH₂-); 1.8 (m, 4H, -CH₂-); 1.05 (t, 6H, -CH₃)

^{13}C -NMR (75 MHz, CDCl_3): δ [ppm] = 164.7 (-COO); 148.8 (py-C); 138.1 (py-C); 127.7 (py-C); 67.7 (-OCH₂-); 22.0 (-CH₂-); 10.4 (-CH₃)

MS (ESI+, masses 40-800): m/z = 525.0 ($[2\text{M}+\text{Na}]^+$, 17%); 311.2 ($[\text{M}+\text{K}]^+$, 24%); 274.2 ($[\text{M}+\text{Na}]^+$, 100%); 252.2 ($[\text{M}+\text{H}]^+$, 39%)

MS/MS (ESI+, masses 40-800, Parent Ion: m/z = 252.2): m/z = 252.2 ($[\text{M}+\text{H}]^+$); 210.1 ($\text{M}^+-\text{H}_2\text{C}=\text{CH}-\text{CH}_3$); 168.0 ($\text{M}^+-2\text{H}_2\text{C}=\text{CH}-\text{CH}_3$)

IR (KBr, 4000-400 cm^{-1}): $\tilde{\nu}$ [cm^{-1}] = 3548 (w), 3078 (w), 2970 (s), 2881 (s), 1720 (s), 1641 (w), 1581 (m), 1460 (m), 1425 (w), 1390 (m), 1350 (w), 1323 (s), 1240 (s), 1140 (s), 1084 (m), 1057 (m), 993 (m), 939 (m), 914 (m)



Diisopropyl-2,6-pyridinedicarboxylate (PDCIPE):

Elemental analysis: C: 61.89% (calc.: 62.14%); H: 6.62% (calc.: 6.82%); N: 5.56% (calc.: 5.57%);

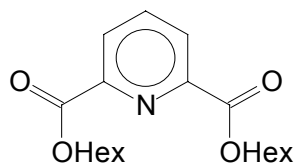
^1H -NMR (300 MHz, CDCl_3): δ [ppm] = 8.2 (d, 2H, py-H); 7.95 (t, 1H, py-H); 5.3 (m, 2H, O-CH-); 1.45 (d, 12H, -CH₃)

^{13}C -NMR (75 MHz, CDCl_3): δ [ppm] = 164.5 (-COO); 149.1 (py-C); 137.9 (py-C); 127.5 (py-C); 70.1 (O-CH); 21.9 (-CH₃)

MS (ESI+, masses 40-800): $m/z = 525.1$ ($[2M+Na]^+$, 24%); 311.2 ($[M+K]^+$, 12%); 274.1 ($[M+Na]^+$, 100%); 252.2 ($[M+H]^+$, 24%)

MS/MS (ESI+, masses 40-800, Parent Ion: $m/z = 252.2$): $m/z = 252.2$ ($[M+H]^+$); 210.1 ($M^+-H_2C=CH-CH_3$); 168.2 ($M^+-2H_2C=CH-CH_3$)

IR (KBr, 4000-400 cm^{-1}): $\tilde{\nu}[cm^{-1}] = 3435$ (w), 3147 (w), 3066 (m), 2989 (m), 2937 (m), 2875 (m), 2062 (w), 1730 (s), 1577 (m), 1454 (m), 1373 (m), 1344 (m), 1290 (s), 1248 (s), 1178 (m), 1144 (m), 1099 (s), 997 (m), 951 (m), 935 (m)



Dihexyl-2,6-pyridinedicarboxylate (PDCHE):

Elemental analysis: C: 68.27% (calc.: 68.03%); H: 8.67% (calc.: 8.71%); N: 4.24% (calc.: 4.18%)

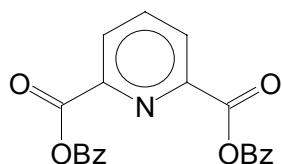
1H -NMR (300 MHz, $CDCl_3$): δ [ppm] = 8.25 (d, 2H, py-H); 8.0 (t, 1H, py-H); 4.45 (t, 4H, -O- CH_2 -); 1.87-1.25 (m, 16H, - CH_2 -); 0.95 (t, 6H, - CH_3)

^{13}C -NMR (75 MHz, $CDCl_3$): δ [ppm] = 164.7 (-COO); 148.8 (py-C); 138.1 (py-C); 127.7 (py-C); 66.4 (-O- CH_2 -); 31.5 (- CH_2 -); 28.6 (- CH_2 -); 25.6 (- CH_2 -); 22.6 (- CH_2 -); 14.0 (- CH_3)

MS (ESI+, masses 40-800): $m/z = 693.3$ ($[2M+Na]^+$, 13%); 395.2 ($[M+K]^+$, 25%); 358.3 ($[M+Na]^+$, 100%); 336.3 ($[M+H]^+$, 18%)

MS/MS (ESI+, masses 40-800, Parent Ion: $m/z = 336.3$): $m/z = 336.3$ ($[M+H]^+$); 252.1 ($M^+ - H_2C=CH-C_4H_9$); 168.2 ($M^+ - 2H_2C=CH-C_4H_9$)

IR (KBr, 4000-400 cm^{-1}): $\tilde{\nu} [cm^{-1}] = 3454$ (w), 3066 (m), 2956 (s), 2927 (m), 2858 (m), 1741 (s), 1577 (m), 1468 (m), 1385 (m), 1290 (s), 1248 (s), 1174 (s), 1155 (m), 1086 (m), 1049 (w), 993 (m), 904 (w)



Dibenzyl-2,6-pyridinedicarboxylate (PDCBAE):

Elemental analysis: C: 72.12% (calc.: 72.61%); H: 4.70% (calc.: 4.93%); N: 4.07% (calc.: 4.03%)

1H -NMR (300 MHz, $CDCl_3$): δ [ppm] = 8.25 (d, 2H, py-H); 7.95 (t, 1H, py-H); 7.55-7.20 (m, 6H, ar-H); 5.45 (s, 2H, -O-CH₂-)

^{13}C -NMR (75 MHz, $CDCl_3$): δ [ppm] = 164.4 (-COO); 148.6 (py-C); 138.1 (py-C); 135.4 (ar-C); 128.6 (ar-C); 128.5 (ar-C); 128.4 (ar-C); 128.0 (py-C); 67.7 (-O-CH₂-)

MS (ESI+, masses 40-800): $m/z = 717.2$ ($[2M+Na]^+$, 14%); 553.5 (15%); 497.4 (15%); 407.1 ($[M+K]^+$, 18%); 370.1 ($[M+Na]^+$, 100%); 348.2 ($[M+H]^+$, 9%); 294.1 (18%)

MS/MS (ESI+, masses 40-800, Parent Ion: $m/z = 348.2$): $m/z = 348.2$ ($[M+H]^+$); 287.1; 256.1 ($M^+ - (Bz)$); 181.2 ($M^+ - (Bz) - (Ph)$); 168.1 ($M^+ - 2(Bz)$)

IR (KBr, 4000-400 cm^{-1}): $\tilde{\nu}[\text{cm}^{-1}] = 3473$ (w), 3060 (m), 3030 (w), 2943 (w), 1753 (s), 1606 (w), 1576 (m), 1498 (m), 1454 (m), 1375 (m), 1292 (m), 1238 (s), 1174 (m), 1155 (m), 1088 (m), 1030 (w), 1007 (m), 901 (w)

Preparation of the solutions

The solutions of terbium trichloride, europium trichloride, dysprosium trichloride and samarium trichloride were prepared with demineralized water. Cesium chloride, yttrium trichloride and the enzyme solutions were made with aqueous bis tris propane buffer (10^{-2} mol/L). 2,6-Pyridinedicarboxylic acid, the esters of 2,6-pyridinedicarboxylic acid and 2,6-pyridinedicarboxaldehyde were dissolved in aqueous bis tris propane buffer (10^{-2} mol/L) with 5 % (v/v) dimethylsulfoxide to ensure sufficient solubility.

Optimization of the PDC/lanthanide(III)-system

Optimization of the lanthanide ion concentration: 75 μL of bis tris propane buffer (10^{-2} mol/L, pH 8.5) were pipetted into each well of two 96 well microplates. Into 8 x 8 wells of each plate, 75 μL of PDC solution ($3 \cdot 10^{-4}$ mol/L, pH 8.5) and into the remaining 4 x 8 wells, 75 μL of buffer were given. Into four rows of the first microplate, Tb(III) solution with the concentrations $3 \cdot 10^{-3}$ mol/L, $6 \cdot 10^{-4}$ mol/L, $3 \cdot 10^{-4}$ mol/L and 10^{-4} mol/L was added into one row each (12 wells). Into the remaining four rows, Eu(III) solution with the same concentration was pipetted. The second plate was treated in the same way except that the Tb(III) and Eu(III) solutions were replaced by Dy(III) and Sm(III) solutions. The fluorescence intensity was measured with a delay time of 50 μs and an integration time of 1 ms.

Excitation wavelength was 280 nm and emission was detected at 545 nm and 615 nm for the first plate and 570 nm and 640 nm for the second plate.

Addition of Cs(I) to investigate the heavy atom effect: 75 μL of PDC solution ($3 \cdot 10^{-4}$ mol/L, pH 8.5) were pipetted into all 96 wells of a microplate. Then, 75 μL of Tb(III) solution ($3 \cdot 10^{-4}$ mol/L) were given into 6 x 8 wells of the plate and the remaining area of 6 x 8 wells was filled with 75 μL of Eu(III) solution (10^{-4} mol/L). Into four columns, 75 μL of buffer were added into each well for the blank. CsCl solution with concentrations of 3 mol/L, 2 mol/L, 1.5 mol/L, 1 mol/L, 0.3 mol/L, 0.1 mol/L, 0.03 mol/L and 0.01 mol/L was pipetted into the wells of the remaining columns (one concentration per row). A second plate was prepared the same way, except that the Tb(III) and Eu(III) solutions were replaced by Dy(III) and Sm(III) solutions. The fluorescence intensity was measured as described above.

Addition of Y(III) ions to investigate the co-fluorescence effect: Two microplates were prepared and treated as described in the paragraph above, but with the Cs(I) solutions being replaced by Y(III) solutions of the following concentrations: 10^{-3} mol/L, 10^{-4} mol/L, $3 \cdot 10^{-5}$ mol/L, 10^{-5} mol/L, $3 \cdot 10^{-6}$ mol/L, 10^{-6} mol/L, $3 \cdot 10^{-7}$ mol/L and 10^{-7} mol/L.

Optimization of the parameters for time-resolved measurements: 75 μL of Tb(III) solution ($3 \cdot 10^{-4}$ mol/L) and Eu(III), Dy(III) and Sm(III) solutions (10^{-4} mol/L) were pipetted into 12 x 2 wells of a 96 well microtitration plate

each. Thereafter, 75 μL of buffer with a pH of 7.5 were added to the 24 wells filled with Tb(III) solution, buffer with a pH of 8.0 to the Eu(III) and Dy(III) wells and buffer with a pH of 8.5 into the Sm(III) wells. Into the remaining four columns of the microplate, another 75 μL of buffer were added in the same way. Then, 75 μL of PDC solution ($3 \cdot 10^{-4}$ mol/L, pH 7.5, 8.0, 8.5) were added into eight columns. The fluorescence intensity of this plate was measured using the following parameters: Excitation wavelength was 280 nm for all measurements. The four emission wavelengths were 545 nm for the Tb(III) filled wells, 615 nm for Eu(III), 570 for Dy(III) and 640 nm for the Sm(III) wells. The integration time for all measurements was 1 ms and the delay times were 0 μs , 10 μs , 20 μs , 30 μs , 40 μs , 50 μs , 75 μs and 100 μs .

Calibration for 2,6-pyridinedicarboxylic acid with lanthanide(III): 75 μL of Tb(III) solution ($3 \cdot 10^{-4}$ mol/L) and Eu(III), Dy(III) and Sm(III) solutions (10^{-4} mol/L) were pipetted into 12 x 6 wells of four 96 well microtitration plates each. The remaining 12 x 2 wells of the plates were filled with 75 μL of demineralized water for the blank. 75 μL of buffer with a pH of 7.5 were added to all wells of the Tb(III) plate, buffer with a pH of 8.0 to the Eu(III) and Dy(III) plates and buffer with a pH of 8.5 to the Sm(III) filled plate. Then, 75 μL of PDC solution with the appropriate pH value and with the following concentrations were pipetted each into one column of every plate: $3 \cdot 10^{-4}$ mol/L, 10^{-4} mol/L, $3 \cdot 10^{-5}$ mol/L, 10^{-5} mol/L, $3 \cdot 10^{-6}$ mol/L, 10^{-6} mol/L, $3 \cdot 10^{-7}$ mol/L, 10^{-7} mol/L, $3 \cdot 10^{-8}$ mol/L, 10^{-8} mol/L, 10^{-9} mol/L and 10^{-10} mol/L.

The wavelength settings were the same as described above. The delay time was 40 μ s, and the integration time was 1 ms.

Calibration for the lanthanide(III) with 2,6-pyridinedicarboxylic acid: The plates for the calibration of the four lanthanides were prepared and treated in the same way as for the calibration of PDC except that the lanthanide(III) solutions were substituted by PDC solution ($3 \cdot 10^{-4}$ mol/L) and vice versa.

Optimization of the PDC/lanthanide(III)/esterase-system

Optimization of the pH: The pH for the esterase reaction was optimized for the model substance diethyl-2,6-pyridinedicarboxylate (PDCEE) for all four lanthanide ions. Tb(III) solution (50 μ L, $3 \cdot 10^{-4}$ mol/L) and Eu(III), Dy(III) and Sm(III) solutions (50 μ L, 10^{-4} mol/L) were pipetted into all 96 wells of four microtitration plates. Then, 50 μ L bis tris propane buffer with a pH of 6.5, 7.0, 7.5, 8.0, 8.5 and 9.0 were given into two columns (for each pH value) of each plate. Thereafter, the esterase solutions (1 u/mL, pH 6.5, 7.0, 7.5, 8.0, 8.5, 9.0) were added in the same way as the buffer solution except that in the last two wells of each column the esterase was substituted by 50 μ L of buffer for the blank. 50 μ L of PDCEE solution in water with 5% (v/v) DMSO ($3 \cdot 10^{-4}$ mol/L) were added subsequently into each well of the four plates. All plates were read out directly after the last pipetting step, and again after 5, 15, 30, 45, 60 and 90 minutes. The wavelength settings were the same as described above. The delay time was 40 μ s and the integration time was 1 ms.

Esterase determination with time-resolved fluorescence: For the esterase determination, eight microplates were prepared for every ester/Tb(III) ($3 \cdot 10^{-4}$ mol/L/ $3 \cdot 10^{-4}$ mol/L) and ester/Eu(III) ($3 \cdot 10^{-4}$ mol/L/ 10^{-4} mol/L) combination. As the dihexyl and the dibenzyl ester of 2,6-pyridinedicarboxylic acid were not soluble in the bis tris propane buffer with 5 % (v/v) dimethylsulfoxide and as more dimethylsulfoxide could not be added due to the sensitivity of the enzymes to organic solvents, it was not possible to use these two esters. The microplates for the remaining esters were pipetted as follows: 50 μ L of the respective ester solution (PDCME, PDCEE, PDCPE, PDCIPE, PDCBE) were given into each well of the plates. Subsequently, 50 μ L of esterase solution (pH 7.5 for Tb(III), 8.0 for Eu(III)) with concentrations of 1, 0.3, 0.1, 0.03, 0.01, $3 \cdot 10^{-3}$, 10^{-3} , $3 \cdot 10^{-4}$, 10^{-4} , $3 \cdot 10^{-5}$ and 10^{-5} mol/L were given into one column each. In the last column, buffer for the blank replaced the esterase solution. For the first of the 8 plates, 50 μ L of lanthanide solution were added into each well immediately, and the fluorescence intensity of the plate was measured directly. The other seven plates were allowed to stand for 5, 15, 30, 45, 60, 90 and 120 minutes, respectively, before lanthanide solution was given onto the plate and the plate was read out. The wavelength and time settings were the same as for the measurements described above.

Investigation on the reactivity of esterases from other sources: In two quartz cuvettes, 1 mL of PDCEE solution (10^{-4} mol/L, pH 7.5) was mixed with 1 mL of Tb(III) solution (10^{-4} mol/L). In the first cuvette, 1 mL of esterase solution (from *Bacillus stearothermophilus*, 0.3 u/mL, pH 7.5) was added. To the second

cuvette, 1 mL of buffer (pH 7.5) was added. The fluorescence intensity of the solutions was measured immediately and after 5, 15, 30, 45, 60, 90 and 120 minutes, respectively. This experiment was repeated for the enzyme esterase from *Bacillus* sp..

Optimization of the PDC/lanthanide(III)/XOD-system

Optimization of the pH: The pH for the measurements with XOD was optimized in the same way as for the esterase reactions, except that the esterase solution was replaced by XOD solution and PDCEE by 2,6-pyridinedicarboxaldehyde (PDCAh). The pH was only optimized for Tb(III) and Eu(III).

XOD determination with time-resolved fluorescence: The determination of XOD with PDCAh was performed in the same way as for the enzyme esterase. The used pH for the Tb(III)/PDCAh/XOD-system was 7.0, and the pH for the Eu(III)/PDCAh/XOD-system was 8.0.

4.4 Results and Discussion

In preliminary investigations, 2,6-pyridinedicarboxylic acid (PDC) was selected as a possible sensitizer for the EALL detection scheme. Close to pH 7, PDC was found to be an excellent sensitizer for Tb(III), a good sensitizer for Eu(III) and a moderate sensitizer for Dy(III) and Sm(III). The excitation and emission spectra of the Tb(III)-PDC complex (10^{-4} mol/L) are presented in figure 4.1:

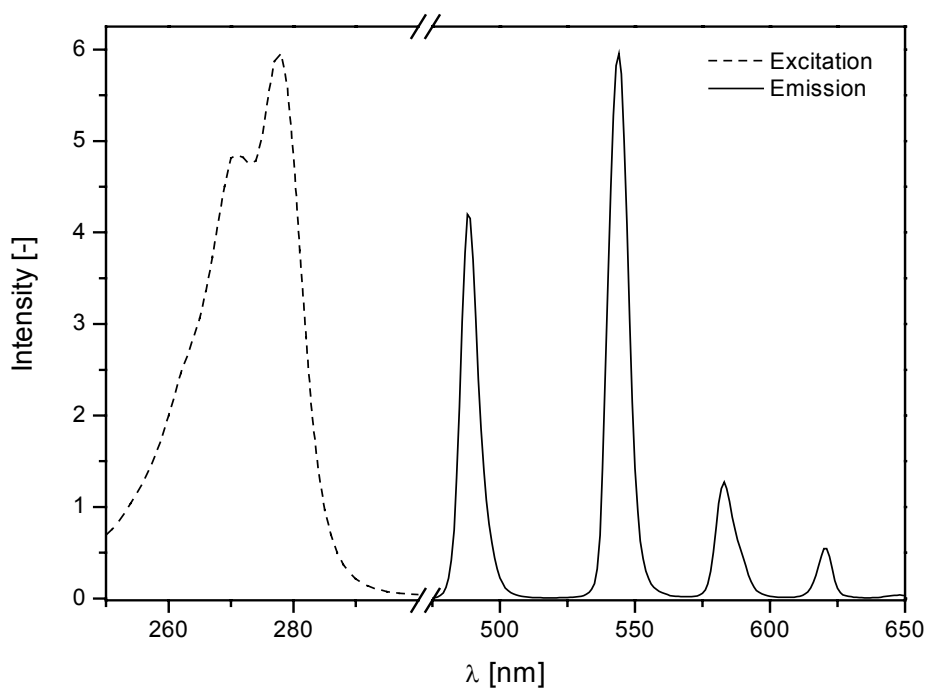


Figure 4.1: Excitation and emission spectra of Tb(III)/PDC (10^{-4} mol/L)

The excitation spectrum (dotted) was recorded using an emission wavelength of 545 nm, the main emission peak of Tb(III). A strong excitation is observed at 278 nm, while the peak shoulder at 272 nm represents the second harmonic of the emission wavelength, which was used for scanning the excitation wavelength. Characteristic for lanthanide emissions, peaks with the typical narrow bandwidths of Tb(III) at maxima of 545, 583 and 620 nm are observed in the spectrum, when using an excitation wavelength of 278 nm. Regarding the respective spectra of the Eu(III)-, Dy(III)- and Sm(III)-PDC complexes, the excitation maximum is located at the same wavelength as for Tb(III)-PDC. The emission maxima are located at the respective characteristic

wavelengths of the individual central ions (Eu(III): 615 and 593 nm, Dy(III): 572 nm and Sm(III): 643 nm).

In the following, the reagent concentrations and other analytical parameters were optimized for the lanthanide-PDC systems: In the presence of a PDC concentration of $3 \cdot 10^{-4}$ mol/L, the concentrations of the lanthanides were varied to investigate the most suitable lanthanide/PDC ratio. The results indicate, as depicted in figure 4.2, that the optimum lanthanide concentration for the Tb(III)-PDC system is $3 \cdot 10^{-4}$ mol/L, while it is 10^{-4} mol/L for all other lanthanide-PDC systems. In the following, these concentrations were used for all other investigations.

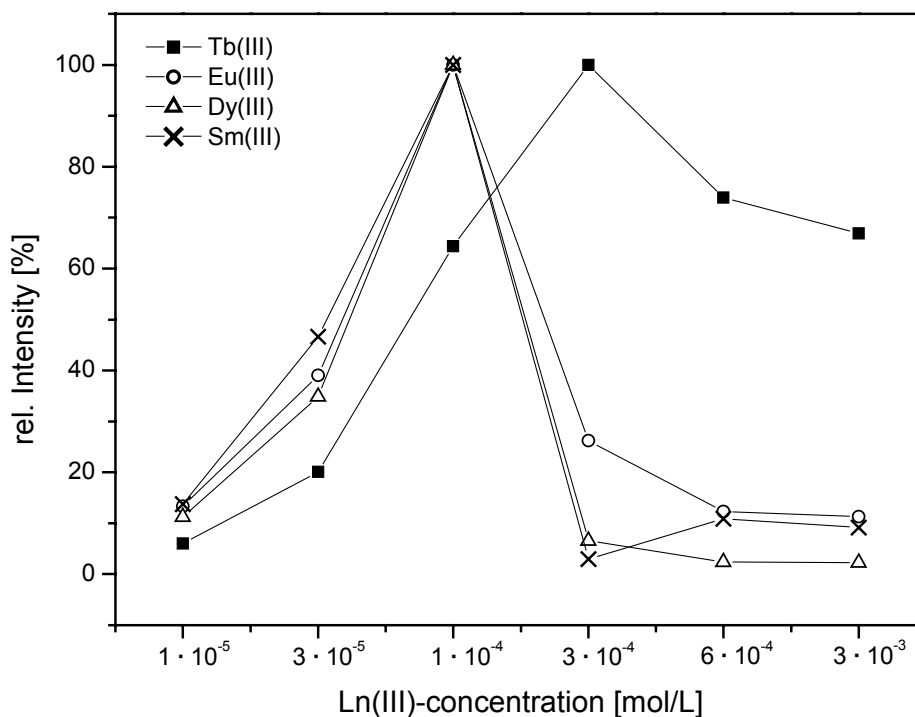


Figure 4.2: Optimization of the lanthanide concentration: Fluorescence signal intensity observed in the presence of 0.3 mol/L PDC

It is known from literature that the presence of high amounts of heavy atoms may facilitate the intersystem crossing (ISC) from the singlet state of the ligand to its triplet state, thus resulting in increased luminescence yields.[6] For this reason, different concentrations of CsCl between 10^{-2} mol/L and 3 mol/L were added, and their influence on the luminescence signal intensity was recorded. The results are depicted in figure 4.3.

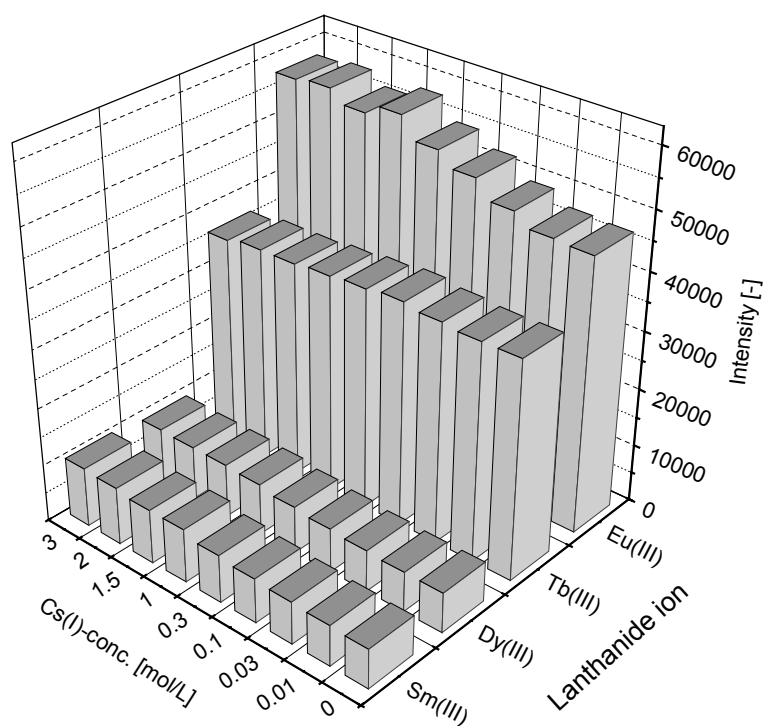


Figure 4.3: Luminescence intensity gain after addition of Cs(I) to the lanthanide(III)/PDC-complexes

As the increase in intensity was only beneficial at high amounts of Cs(I) for the Eu(III)/PDC-complex, negligible for the Sm(III)- and Dy(III)-complexes and even negative for the Tb(III)-complex, all further measurements were carried out without heavy atom salts, with respect to the negative effects of the presence of high amounts of Cs(I) on the used enzyme. Similar

measurements were performed with respect to possible co-luminescence effects of Y(III) ions, which are known to have similarly positive effects in some cases.[7] Due to the fact that only negative effects were observed for Y(III) concentrations between 10^{-7} mol/L and 10^{-3} mol/L, the further use of Y(III) salts was omitted as well.

Time-resolved fluorescence measurements may be advantageous in order to reduce background signals, thus improving limits of detection. Therefore, decay curves for the lanthanide/PDC complexes were recorded by applying different delay times between 0 and 100 μ s and a constant integration time of 1 ms. The results are presented in figure 4.4, and they prove that, in accordance with literature data on other lanthanide complexes, the luminescence of the Tb(III) and Eu(III) complexes is characterized by very long lifetimes, while Dy(III) and Sm(III) complexes decay much faster.

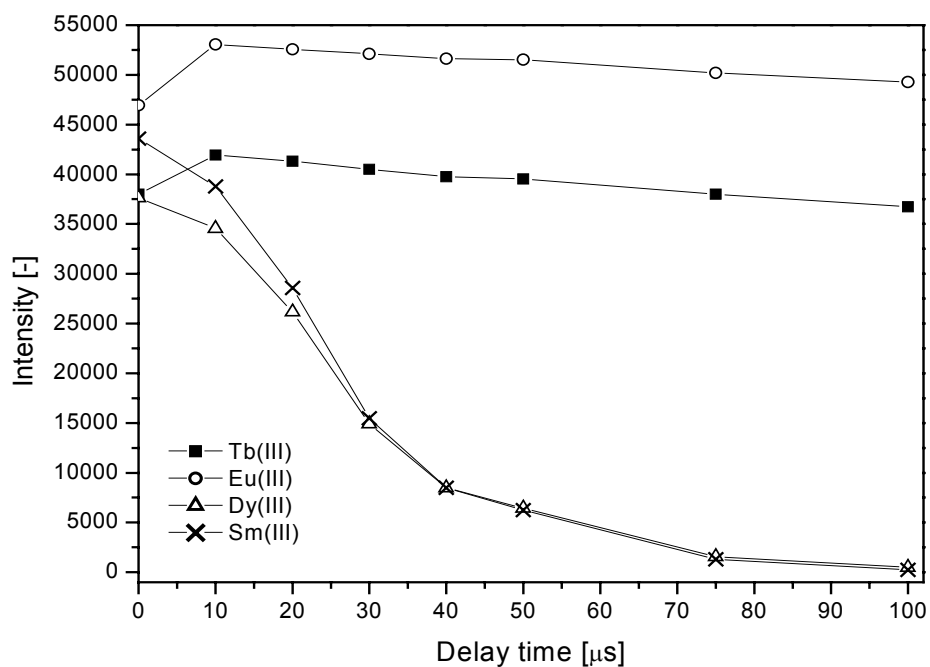


Figure 4.4: Decay curves for different lanthanide/PDC complexes

In the following measurements, a delay time of 40 μs was selected because at this time the background luminescence for all lanthanide/PDC complexes had already been decayed. The integration time of 1 ms was kept constant for all complexes.

Using the optimized parameters, the analytical figures of merit for the determination of the lanthanides and of PDC were recorded. The respective results for the analysis of the lanthanides are presented in table 4.1, while the data for the determination of PDC can be found in table 4.2.

Table 4.1: LOD and LOQ for the determination of Tb(III) and Eu(III) using PDC ($c(\text{PDC}) = 3 \cdot 10^{-4} \text{ mol/L}$)

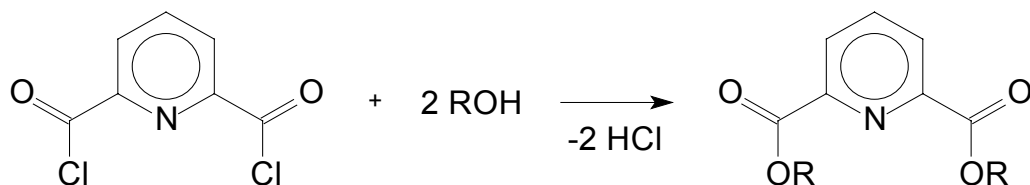
Lanthanide(III)	LOD [mol/L]	LOQ [mol/L]
Tb(III)	10^{-7}	$3 \cdot 10^{-7}$
Eu(III)	10^{-7}	$3 \cdot 10^{-7}$
Dy(III)	10^{-5}	$3 \cdot 10^{-5}$
Sm(III)	-	-

Table 4.2: LOD and LOQ for the determination of PDC using different lanthanides ($c(\text{Tb(III)}) = 3 \cdot 10^{-4} \text{ mol/L}$; $c(\text{Eu(III)}, \text{Dy(III)}, \text{Sm(III)}) = 10^{-4} \text{ mol/L}$)

Lanthanide(III)	Tb(III)	Eu(III)	Dy(III)	Sm(III)
LOD [mol/L]	10^{-7}	10^{-6}	$3 \cdot 10^{-5}$	-
LOQ [mol/L]	$3 \cdot 10^{-7}$	$3 \cdot 10^{-6}$	10^{-4}	-

Similar limits of detection (LOD) and limits of quantification (LOQ) are obtained for Tb(III) and Eu(III). While the LOD for Dy(III) is already inferior by a factor of 100, no useful results were obtained for Sm(III) owing to low luminescence intensities. For the determination of PDC, best results were obtained with Tb(III), and the limit of detection in the presence of Eu(III) is already inferior by one order of magnitude. Therefore, Tb(III) was selected as preferred lanthanide cation for all further measurements. It should be noted that the data were obtained using an older generation filter-based microplate reader and that the limits of detection could possibly be improved with state-of-the-art instrumentation.

After the optimization of the detection parameters, different EALL applications should be developed based on the Tb(III)-PDC system. The major focus should be directed to one hydrolytic enzyme and one redox enzyme. Esterase was selected as hydrolytic enzyme, and the respective PDC diesters of various alcohols were synthesized to provide a large selection of possible substrates. Apart from the commercially available methyl, ethyl and butyl esters of PDC, the esters of propanol, isopropanol, hexanol and benzyl alcohol were synthesized by alcoholysis of the PDC dichloride according to figure 4.5. The characterization of the products is described in Chapter 4.3



ROH = 1-propanol, 2-propanol, 1-hexanol, benzylalcohol

Figure 4.5: *Synthesis of the PDC esters*

As the polarity of the esters is low, investigations were carried out in order to find a suitable compromise between the solubility in aqueous or aqueous/organic media and sufficient enzymatic activity. A content of 5% (v/v) of dimethylsulfoxide in the ester solutions of aqueous buffer did not reduce the esterase activity significantly. However, the PDC esters of hexanol and benzyl alcohol required a significantly higher organic content to achieve solubility. For this reason, the subsequent investigations were carried out exclusively for the esters of the alcohols with alkyl chain lengths between one and four carbon

atoms. In figure 4.6, the enzymatic cleavage of the PDC esters and the subsequent complexation with the Ln(III) ions are shown.

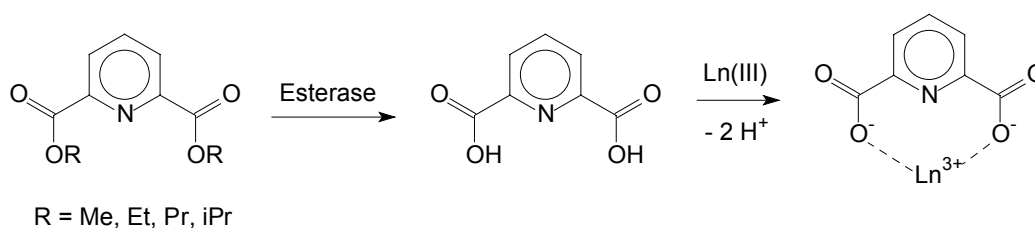


Figure 4.6: Hydrolysis and subsequent complexation of the PDC esters

In the following, the pH dependency of the enzymatic reaction was investigated with respect to all four lanthanide cations: In the pH range between 6.5 and 9 with a resolution of 0.5 pH units, bis tris propane buffer was used. The results are presented in figure 4.7.

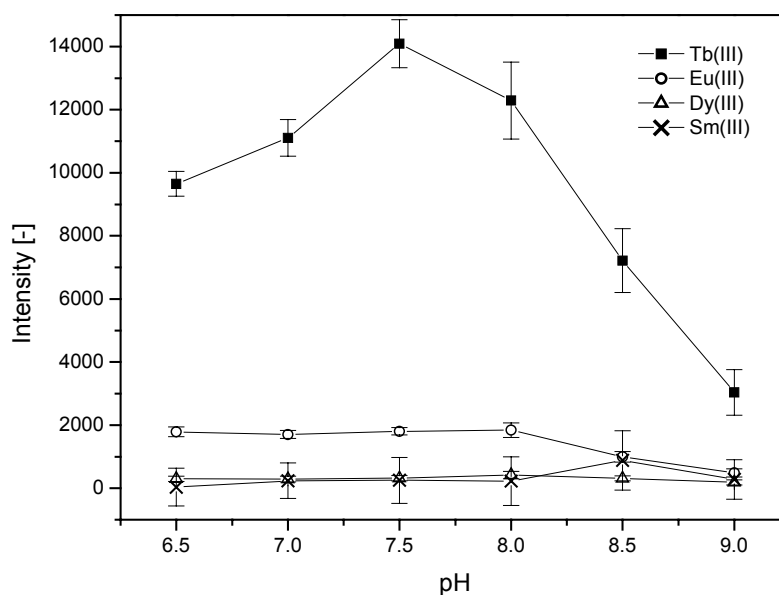


Figure 4.7: Investigation on the pH dependency of the esterase-catalyzed cleavage of the ethyl ester of PDC and the complexation/energy transfer for different lanthanides (the error bars represent the standard deviation of the fluorescence intensity ($n = 12$))

The enzymatic reaction with subsequent Tb(III) complexation yields best results at pH 7.5, while the Eu(III)- and Dy(III)-PDC systems have their optimum pH at 8.0, and the Sm(III)-PDC even at pH 8.5. As could already be expected from the earlier optimization of the detection conditions, best results are also obtained for Tb(III) compared with the other lanthanides.

The velocity of the enzymatic conversion was tested for different esters. In figure 4.8, the progress of the reaction in the presence of 0.3 u/mL of esterase from porcine liver is presented for different esters. Tb(III) was added, and the time-resolved luminescence was measured as described above. The blank values (identical measurements, but without enzymatic catalysis are subtracted).

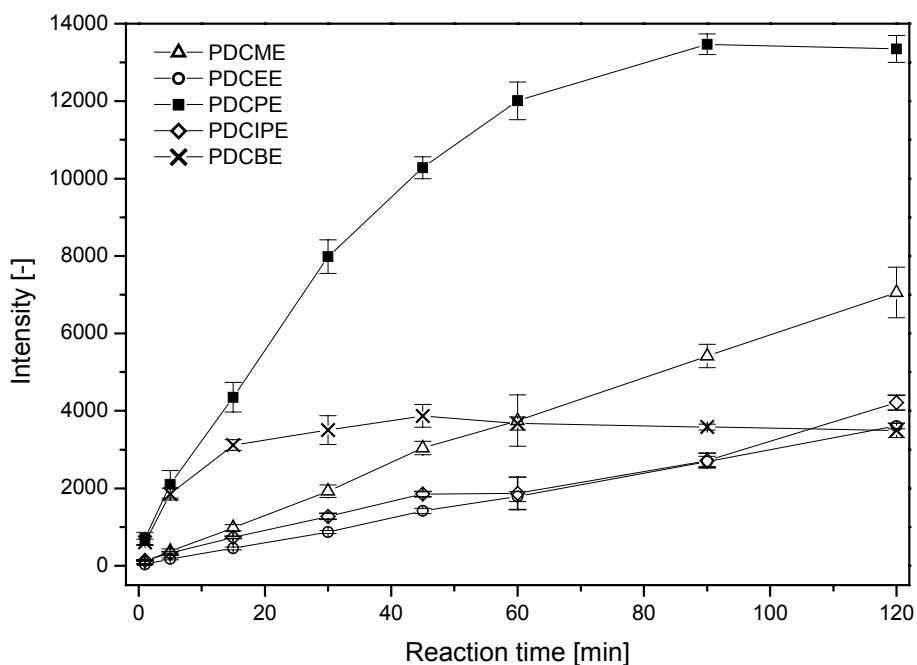


Figure 4.8: Progress of the enzymatic reaction for the Tb(III)-PDC system using different esters. The error bars represent the standard deviation of the fluorescence intensity ($n = 8$)

The fastest conversion is observed for the propyl ester, while the butyl ester reacts slower and shows a higher tendency to be decomposed already without catalyst, thus resulting in higher background signals. The latter becomes obvious from the decreasing intensity values at very long reaction times, which are due to the subtraction of an increasing blank from an almost constant signal of the butyl ester cleavage. The slow conversion of the ethyl ester is not fully understood and requires further investigations. In contrast, the same effect for the isopropyl ester can be traced back to sterical reasons. The cleavage of the methyl ester proceeds slowly, but steadily with comparably low blank. Therefore, the propyl ester is most attractive for future applications. The data for LOD and LOQ in the determination of esterase have been determined using these esters in combination with Tb(III)/Eu(III) and are summarized in table 4.3.

Table 4.3: LOD and LOQ for the determination of esterase using different esters and lanthanides ($c(\text{Tb(III)}) = 3 \cdot 10^{-4} \text{ mol/L}$, $c(\text{Eu(III)}) = 10^{-4} \text{ mol/L}$; reaction time: 120 min)

Ester	Tb(III)		Eu(III)	
	LOD [u/mL]	LOQ [u/mL]	LOD [u/mL]	LOQ [u/mL]
PDCME ($3 \cdot 10^{-4} \text{ mol/L}$)	10^{-2}	$3 \cdot 10^{-2}$	$3 \cdot 10^{-2}$	0.1
PDCEE ($3 \cdot 10^{-4} \text{ mol/L}$)	$3 \cdot 10^{-3}$	10^{-2}	$3 \cdot 10^{-2}$	0.1
PDCPE ($3 \cdot 10^{-4} \text{ mol/L}$)	10^{-3}	$3 \cdot 10^{-3}$	$3 \cdot 10^{-3}$	10^{-2}
PDCIPE ($3 \cdot 10^{-4} \text{ mol/L}$)	10^{-2}	$3 \cdot 10^{-2}$	10^{-2}	$3 \cdot 10^{-2}$
PDCBE (10^{-4} mol/L)	$3 \cdot 10^{-3}$	10^{-2}	10^{-3}	$3 \cdot 10^{-3}$

As could be expected from the reaction velocity, the propyl ester in combination with Tb(III) yields the best results. Surprisingly, the same figures of merit are achieved for the combination of the butyl ester and Eu(III). In general, the performance of the Eu(III) systems is improving with increasing chainlength of the esters.

Esterases from other sources were investigated, too. For those investigations, an esterase from bacillus stearothermophilus and an esterase from bacillus sp. have been treated in the same way as the esterase from porcine liver with the exception that those studies have been performed in cuvettes and not on microplates. It was found that the esterase from bacillus stearothermophilus showed a catalytic activity whereas the esterase from bacillus sp. did not react at all. Further investigations have to be performed concerning the selectivity of the substrate.

As a second enzymatic conversion, the XOD-catalyzed reaction of 2,6-pyridinedicarboxaldehyde under formation of PDC was investigated. The involved reactions are depicted in Figure 4.9.

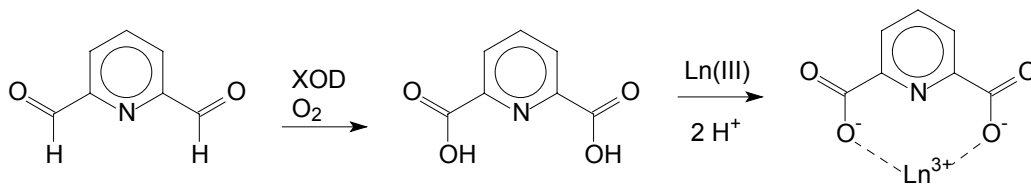


Figure 4.9: XOD-catalyzed oxidation of 2,6-pyridinedicarboxaldehyde and subsequent complexation

The optimization of the pH for the enzymatic conversion and the complexation were carried out as in the case of esterase from porcine liver. Figure 4.10 shows that the optimum pH in the presence of Tb(III) is 7.0, while the optimum pH in the presence of Eu(III) is 8.0. Figure 4.11 depicts the time trace of the enzymatic conversion of PDCAh to PDC with Tb(III) and Eu(III).

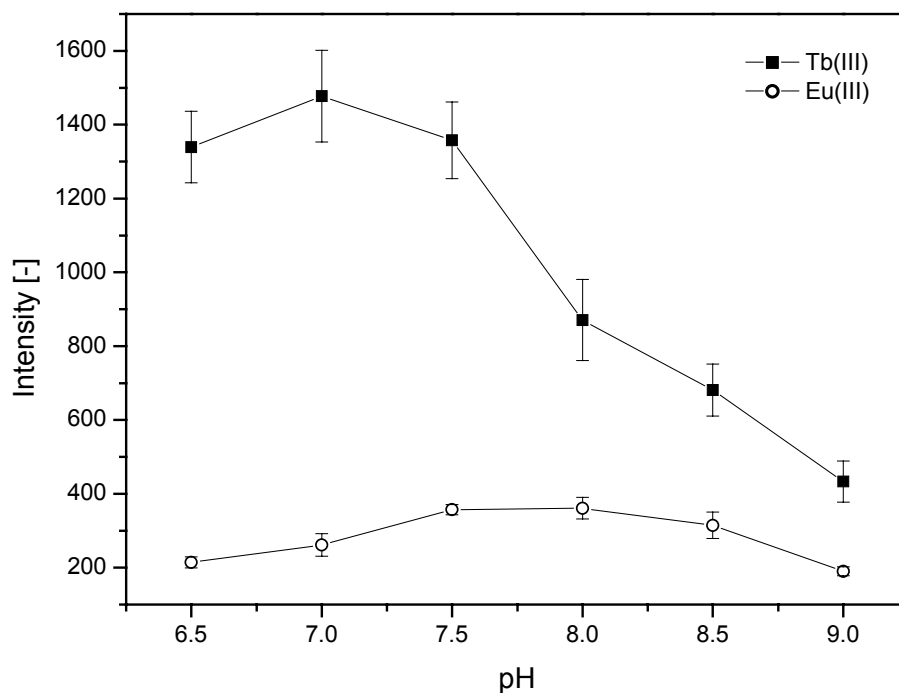


Figure 4.10: Investigation on the pH dependency of the XOD-catalyzed reaction and energy transfer for Tb(III) and Eu(III) (the error bars represent the standard deviation of the fluorescence intensity ($n = 12$))

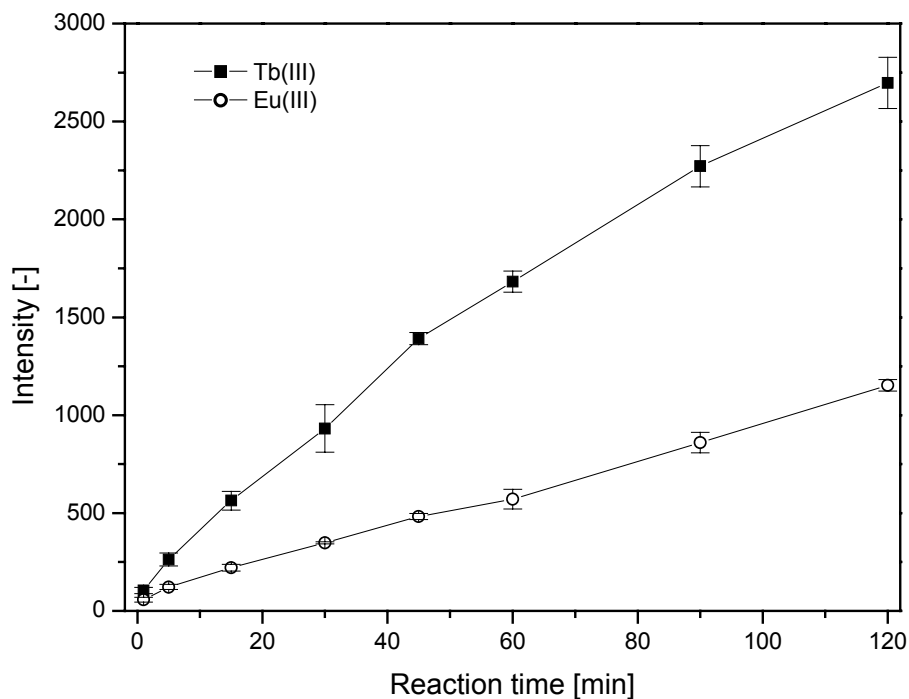


Figure 4.11: Time trace of the enzymatic conversion of PDCAh ($3 \cdot 10^{-4}$ mol/L) to PDC with Tb(III) ($3 \cdot 10^{-4}$ mol/L) and Eu(III) ($3 \cdot 10^{-4}$ mol/L) at a XOD concentration of 0.3 u/mL

The analytical figures of merit for the XOD system in combination with Tb(III) and Eu(III) are presented in Table 4.4. For Tb(III), the obtained LOD and LOQ are superior by a factor of three compared to Eu(III).

Table 4.4: LOD and LOQ for the determination of XOD using 2,6-pyridinedicarboxaldehyde in combination with Tb(III) and Eu(III) ($c(\text{Tb(III)}) = 3 \cdot 10^{-4}$ mol/L; $c(\text{Eu(III)}, \text{Dy(III)}, \text{Sm(III)}) = 10^{-4}$ mol/L)

Ln(III)	Tb(III)	Eu(III)	Dy(III)	Sm(III)
LOD [mol/L]	10^{-7}	10^{-6}	$3 \cdot 10^{-5}$	-
LOQ [mol/L]	$3 \cdot 10^{-7}$	$3 \cdot 10^{-6}$	10^{-4}	-

4.5 Conclusions

Within this chapter, the suitability of the lanthanide/PDC system for EALL detection has been proven for one hydrolytic enzyme and one redox enzyme. The measurements were performed close to the physiological pH, and therefore no co-ligand had to be added. Future work may be directed to the development of assay applications and to the further expansion of the system to other groups of enzymes, e.g., proteases.

4.6 References

- [1] Gudgin Dickson, E. F.; Pollak, A.; Diamandis, E. P. *Pharmacol. Therapeut.* **1995**, 66, 207-235
- [2] Elbanowski, M.; Makowska, B. *J. Photoch. Photobio. A* **1996**, 99, 85-92
- [3] Heinonen, P.; Iitiä, A.; Torresani, T.; Lövgren T. *Clin. Chem.* **1997**, 43, 1142-1150
- [4] Meyer, J.; Karst, U. *Analyst* **2000**, 125, 1537-1538
- [5] Jenkins, A. L.; Murray, G. M. *Anal. Chem.* **1996**, 68, 2974–2980
- [6] Zhu, R.; Kok, W. T. *Anal. Chem.* **1997**, 69, 4010–4016
- [7] Xu, Y. Y.; Lövgren, T.; Hemmilä, I. A. *Analyst* **1992**, 117, 1061-1069

Lanthanide-catalyzed hydrolysis of 4,7-diphenyl-1,10-phenanthroline-2,9-dicarboxylic acid esters

5.1 Abstract

It is known from literature that 4,7-diphenyl-1,10-phenanthroline-2,9-dicarboxylic acid (DPPDA) and its derivatives are outstanding sensitizers for Eu(III) ions and basing on this ligand a new EALL system should be developed. This compound can be considered to be a higher homologue of 2,6-pyridinedicarboxylic acid (PDC), for which the EALL method development was described in chapter 4. PDC could already be applied for the determination of esterase and XOD and DPPDA was expected to be an even more promising candidate for the development of a more powerful EALL detection scheme, due to the greater complexation capacity and due to the high luminescence yield that DPPDA exhibits when complexed to Eu(III).

*Steinkamp, T.; Hayen, H.; Karst, U. submitted for publication to *Chemical Communications*

5.2 Introduction

In 1988, Diamandis et al. published a paper in which they describe the synthesis of 4,7-bis-chlorosulfophenyl-1,10-phenanthroline-2,9-dicarboxylic acid (BCPDA), an outstanding sensitizer for Eu(III), and the labeling of BSA with this ligand.[1] In the future it was established as marker in bioassays for various different analytes.[2-4] The ligand exhibits a remarkable high binding capacity to the complexed ions, which is due to four possible complexation sites (two N-atoms of the phenanthroline and two O-atoms of the two carboxylic acid moieties). Another advantage of BCPDA is the large luminescence yield, which is achieved by its Eu(III) complex at nearly neutral pH (no addition of EDTA necessary).

Due to those features, it was decided to develop an EALL system employing DPPDA. Initial work consisted of the synthesis of various esters of DPPDA. First measurements showed a strong increase of the fluorescence intensity at 612 nm when combining an ester, an esterase and Eu(III) ions in aqueous/organic solutions at neutral pH as expected. The results indicated that cleavage of the esters takes place under formation of the free acids, which transfer previously absorbed energy to the lanthanide ions. Surprisingly, and in contrast to earlier experiments using the PDC esters, blank experiments rapidly proved that the same reaction was observed as well in the absence of an esterase.

This initiated a further series of experiments and an intense literature search to elucidate the nature of the unexpected phenomenon. The experiments

indicated that the Eu(III) exhibits a significant catalytic activity on this reaction and it was found that the Eu(III)-catalyzed cleavage of phosphate esters and of DNA is known in literature since long.[5,6] Recently, Brown et al. published several papers on the methanolysis of various esters and lactams under catalysis of Eu(III), La(III), Zn(II) and Co(II) in non-aqueous solutions.[7, 8] Up to now, only Takarada et al. described the lanthanide ion-induced hydrolyses of alkyl esters and amides of α -amino acids.^[10] They suggest a two-step reaction sequence with involvement of the amino group of the respective amino acid.

5.3 Experimental Section

Chemicals

All chemicals were, if not mentioned otherwise, purchased in the highest purity available: Bathocuproine, ammonium formate, Y(III) trichloride hexahydrate and the following lanthanide(III) trichloride hexahydrates were obtained from Aldrich (Steinheim, Germany): Nd(III), Sm(III), Eu(III), Gd(III), Tb(III), Dy(III) and Yb(III). Benzoylperoxide (75%), Al(III) trichloride hexahydrate, Fe(III) trichloride hexahydrate and the following lanthanide(III) trichloride hexahydrates were purchased at Acros (Geel, Belgium): La(III), Ce(III), Pr(III), Ho(III), Er(III), Tm(III) and Lu(III). DMSO, formic acid and the dried alcohols for the ester synthesis were from Merck (Darmstadt, Germany), *n*-chlorosuccinimide (96%) from Fluka (Neu-Ulm, Germany) and bis tris propane (1,3-bis[tris(hydroxymethyl)methylamino]propane) from Sigma (Deisenhofen, Germany). The employed solvents for the LC-MS

measurements were LC-MS grade from BioSolve (Valkenswaard, The Netherlands).

Instrumentation

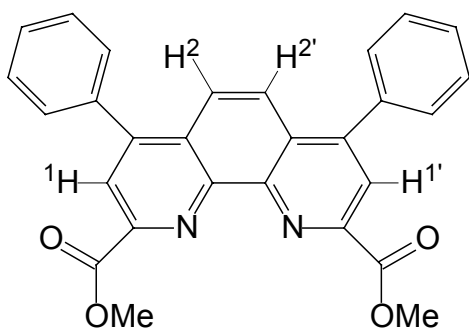
The fluorescence measurements were performed using a fluorescence spectrometer AMINCO-Bowman series 2 from Polytec GmbH (Waldbronn, Germany) with AB 2 software version 5.00. For all measurements, a spectral bandwidth of 4 nm was applied.

For the LC-MS setup, an Agilent Technologies HP1100 liquid chromatograph for binary gradient elution, including an autosampler and a diode array detector, was coupled to an esquire 3000*plus* ion trap mass spectrometer from Bruker Daltonics, equipped with an electrospray ionization (ESI) interface.

Synthesis and characterization of the DPPDA esters

The synthesis of 4,7-diphenyl-1,10-phenanthroline-2,9-dicarboxylic acid and its dimethyl ester were described by Diamandis et al..[1] To the best of our knowledge, the other esters synthesized and used by our group have not been described before. The synthesis of the diethyl, dipropyl and diisopropyl esters of 4,7-diphenyl-1,10-phenanthroline-2,9-dicarboxylic acid were performed according to this description.

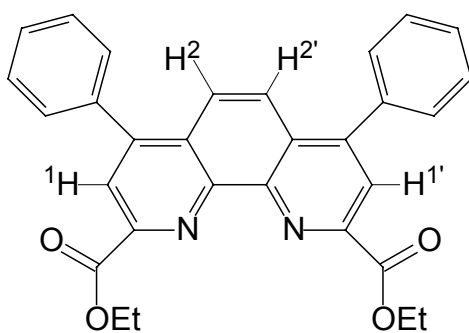
The obtained esters were characterized in the following by means of ESI-MS and $^1\text{H-NMR}$:



4,7-Diphenyl-1,10-phenanthroline-2,9-dicarboxylic acid dimethyl ester (DPPDAME):

$^1\text{H-NMR}$ (300 MHz, CDCl_3): δ [ppm] = 8.45 (s, 2H, 1/1'); 8.05 (s, 2H, 2/2'); 7.55 (s, 10H, Ph-H); 4.15 (s, 6H, $-\text{CH}_3$)

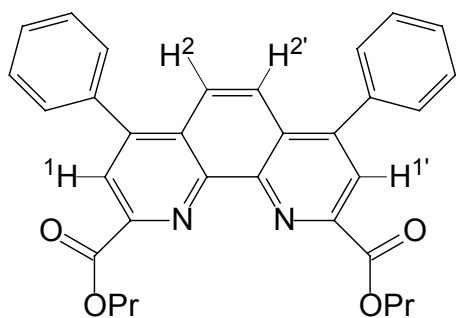
MS (ESI+, masses 50-800): m/z = 487.1 ($[\text{M}+\text{K}]^+$, 15%); 471.1 ($[\text{M}+\text{Na}]^+$, 100%); 449.1 ($[\text{M}+\text{H}]^+$, 73%)



4,7-Diphenyl-1,10-phenanthroline-2,9-dicarboxylic acid diethyl ester (DPPDAEE):

$^1\text{H-NMR}$ (300 MHz, CDCl_3): δ [ppm] = 8.45 (s, 2H, 1/1'); 8.05 (s, 2H, 2/2'); 7.55 (s, 10H, Ph-H); 4.6 (q, 4H, $-\text{CH}_2-$); 1.6 (t, 6H, $-\text{CH}_3$)

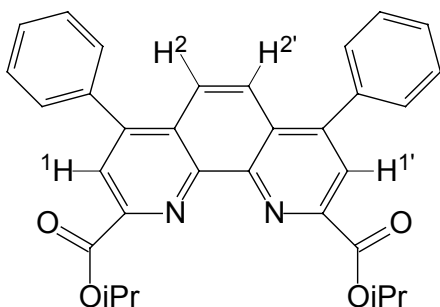
MS (ESI+, masses 50-800): m/z = 515.0 ($[\text{M}+\text{K}]^+$, 12%); 499.2 ($[\text{M}+\text{Na}]^+$, 100%); 477.2 ($[\text{M}+\text{H}]^+$, 87%)



4,7-Diphenyl-1,10-phenanthroline-2,9-dicarboxylic acid dipropyl ester (DPPDAPE):

$^1\text{H-NMR}$ (300 MHz, CDCl_3): δ [ppm] = 8.4 (s, 2H, 1/1'); 8.0 (s, 2H, 2/2'); 7.55 (s, 10H, Ph-H); 4.5 (t, 4H, O- CH_2 -); 2.0 (m, 4H, - CH_2 -); 1.1 (t, 6H, - CH_3)

MS (ESI+, masses 50-800): m/z = 543.1 ($[\text{M}+\text{K}]^+$, 6%); 527.2 ($[\text{M}+\text{Na}]^+$, 100%); 505.2 ($[\text{M}+\text{H}]^+$, 96%)



4,7-Diphenyl-1,10-phenanthroline-2,9-dicarboxylic acid diisopropyl ester (DPPDAiPE):

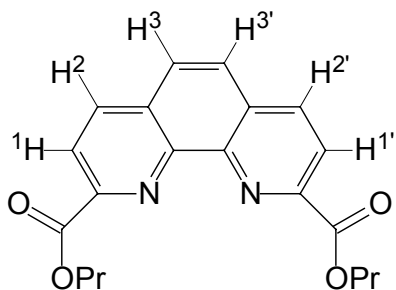
$^1\text{H-NMR}$ (300 MHz, CDCl_3): δ [ppm] = 8.4 (s, 2H, 1/1'); 8.0 (s, 2H, 2/2'); 7.55 (s, 10H, Ph-H); 5.45 (m, 2H, -CH); 1.55 (d, 12H, - CH_3)

MS (ESI+, masses 50-800): m/z = 543.1 ($[\text{M}+\text{K}]^+$, 2%); 527.2 ($[\text{M}+\text{Na}]^+$, 100%); 505.2 ($[\text{M}+\text{H}]^+$, 97%)

Synthesis and characterization of the 1,10-phenanthroline-2,9-dicarboxylic acid dipropyl ester

To a mixture of 488 mg (2 mmol) 1,10-phenanthroline-2,9-dicarboxylic acid in 5 mL propanol, 90 μ L sulfuric acid (conc.) were added. The mixture was refluxed for 4 h under stirring. After concentration at the rotary evaporator, diethylether was added and the solution was de-acidified with a concentrated solution of Na_2CO_3 . The organic phase was dried subsequently with Na_2SO_4 and the solvent was removed by means of vacuum evaporation. The remaining compound was recrystallized from hot propanol/ethyl acetate/dichloromethane in equal shares.

The obtained ester was characterized in the following by means of ESI-MS and $^1\text{H-NMR}$:



1,10-phenanthroline-2,9-dicarboxylic acid dipropyl ester:

$^1\text{H-NMR}$ (300 MHz, CDCl_3): δ [ppm] =
 8.45 (m, 4H, 1/1'/2/2'); 7.95 (s, 2H, 3/3');
 4.5 (t, 4H, O- CH_2 -); 2.0 (m, 4H, - CH_2 -);
 1.05 (t, 6H, - CH_3)

MS (ESI+, masses 50-800): m/z = 391.1 ($[\text{M}+\text{K}]^+$, 1%); 375.2 ($[\text{M}+\text{Na}]^+$, 3%);
 353.2 ($[\text{M}+\text{H}]^+$, 100%)

Time dependent luminescence measurements of the ester cleavage with different Eu(III) concentrations

1 mL of ester solution in DMSO (10^{-5} mol/L) was transferred into two fluorescence cuvettes each and 250 μ L of aqueous bis tris propane buffer solution (10^{-2} mol/L, pH 7.4) were added. Subsequently, 250 μ L of aqueous Eu(III) solution (10^{-3} mol/L or 10^{-5} mol/L, respectively) were pipetted into the cuvettes. The luminescence intensity in the cuvettes (excitation wavelength: 339nm, emission wavelength: 612nm) was measured immediately and repeatedly at defined time intervals.

Investigations on the temperature dependency of the catalysis

For every DPPDA ester three cuvettes were filled as follows: 400 μ L of ester solution in DMSO (10^{-4} mol/L) were given into all three cuvettes that already contained 800 μ L DMSO. Then, 400 μ L of aqueous bis tris propane buffer solution (10^{-2} mol/L, pH 7.4) were added. Into all three cuvettes 400 μ L of aqueous Eu(III) solution (10^{-3} mol/L) were pipetted. The cuvettes for the blank measurements were treated identically, with the only exception that the Eu(III) solution was only added shortly before each measurement. One measurement cuvette and its blank cuvettes were then kept at room temperature, the cuvettes for the second test series at 50 $^{\circ}$ C and the last cuvettes at 80 $^{\circ}$ C. The luminescence intensity of all measurement cuvettes and their respective blank cuvettes (excitation wavelength: 339nm, emission wavelength: 612nm) was measured immediately and repeatedly at defined time intervals.

Investigations on the catalytic activity of various lanthanide(III) ions, Fe(III), Al(III) and Y(III) by means of ESI-MS

An aqueous 10^{-3} mol/L ion(III) chloride solution (300 μ L) was added to 1200 μ L of a solution of DPPDA dimethyl ester in acetonitrile (10^{-5} mol/L). 5 μ L of this reaction mixture were then directly injected into the LC-MS system. The injection was repeated subsequently every 4 minutes. All substances were detected as $[M+H]^+$ pseudomolecular ions and their sodium adducts in the positive ionization mode. The solvent stream of the LC consisted of 30 % of aqueous formic acid buffer pH 3 and 70 % acetonitrile at a flow rate of 0.3 mL/min.

Investigation on the Eu(III)-catalyzed methanolysis of the DPPDA dipropyl ester

An aqueous $2 \cdot 10^{-5}$ mol/L Eu(III) chloride solution (300 μ L) was added to a mixture of 600 μ L DPPDA dipropyl ester solution in acetonitrile (10^{-5} mol/L) and 600 μ L methanol. The measurements were performed as described above.

5.4 Results and Discussion

The various DPPDA esters and DPPDA itself were synthesized in a two-step reaction sequence, which is depicted in figure 5.1:

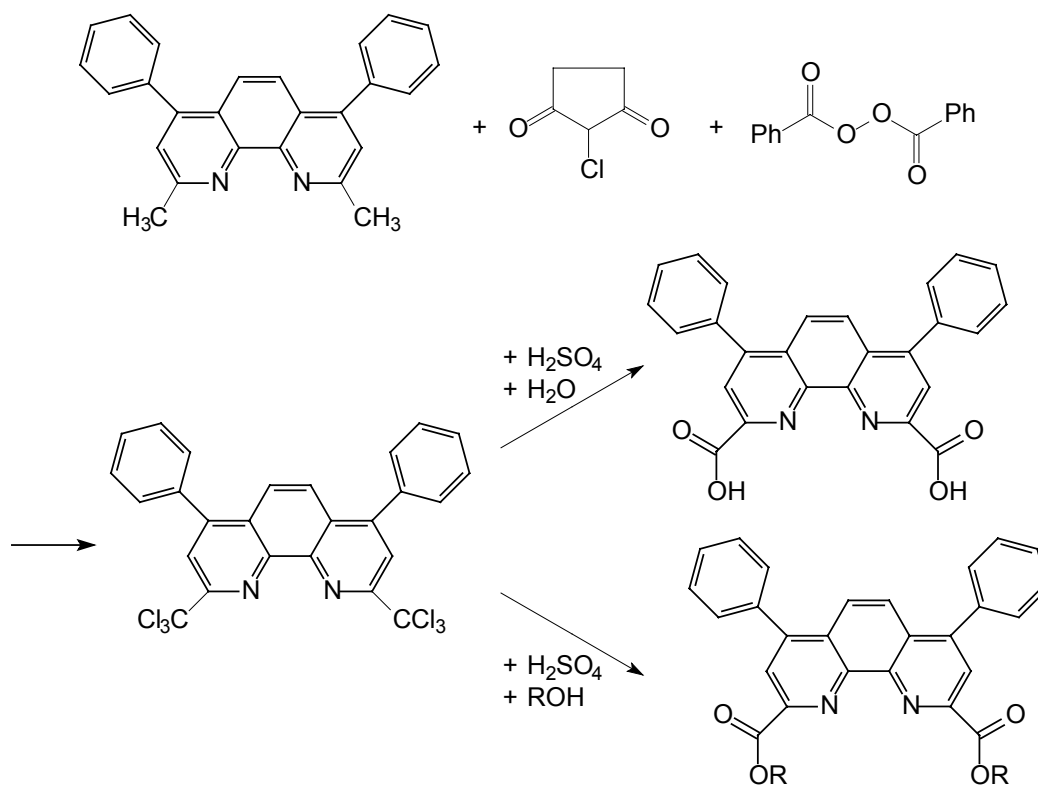


Figure 5.1: Reaction sequence yielding DPPDA and its esters starting from bathocuproine

As can be seen in figure 5.1, the reaction sequence starts with the commercially available bathocuproine, which is chlorinated in the presence of *n*-chlorosuccinimide and benzoyl peroxide. The intermediate can either react to DPPDA when heated in sulfuric acid in the presence of water or to the esters of DPPDA in the presence of an alcohol. For this work the dimethyl-, diethyl-, dipropyl- and diisopropyl ester were synthesized according to this procedure.

All initial investigations concerning the Eu(III) catalyzed DPPDA ester cleavage were carried out by lanthanide luminescence. The reaction scheme

is presented in figure 5.2, and the fluorescence spectrum of the resulting Eu(III)/DPPDA complex is presented in Figure 5.3.

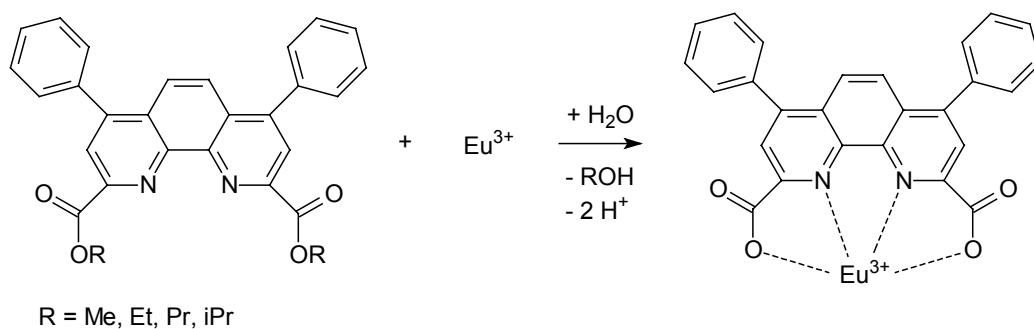


Figure 5.2: Reaction scheme of the Eu(III) catalyzed ester cleavage of the esters of DPPDA

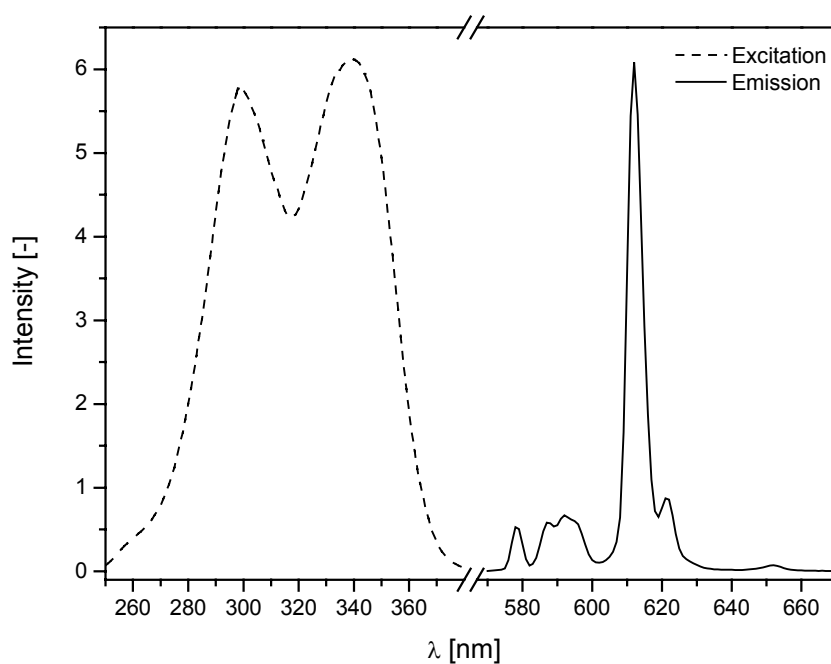


Figure 5.3: Excitation and emission spectra of the DPPDA/Eu(III) complex

It is obvious that upon excitation of the ligand at 339 nm, strong emission of the central ion at 612 nm is observed.

An explanation for the differences observed between the PDC esters (no hydrolysis catalyzed by Eu(III)) and DPPDA esters (strong hydrolysis) could be the stronger complexation, which can be expected from the DPPDA esters (two tertiary nitrogen atoms in the phenanthroline ring may serve as electron donors) in contrast to the PDC esters (one electron donor in the pyridine ring). This way, Eu(III) is bound close to the ester groups of DPPDA and has improved possibilities to interact with these. For all DPPDA esters, a strong catalytic effect of Eu(III) was observed, with the strongest for the dimethyl ester, followed by the dipropyl and diethyl esters. As could be expected, the cleavage of the sterically hindered diisopropyl ester of DPPDA was significantly slower. These data are presented in detail in Figure 5.4:

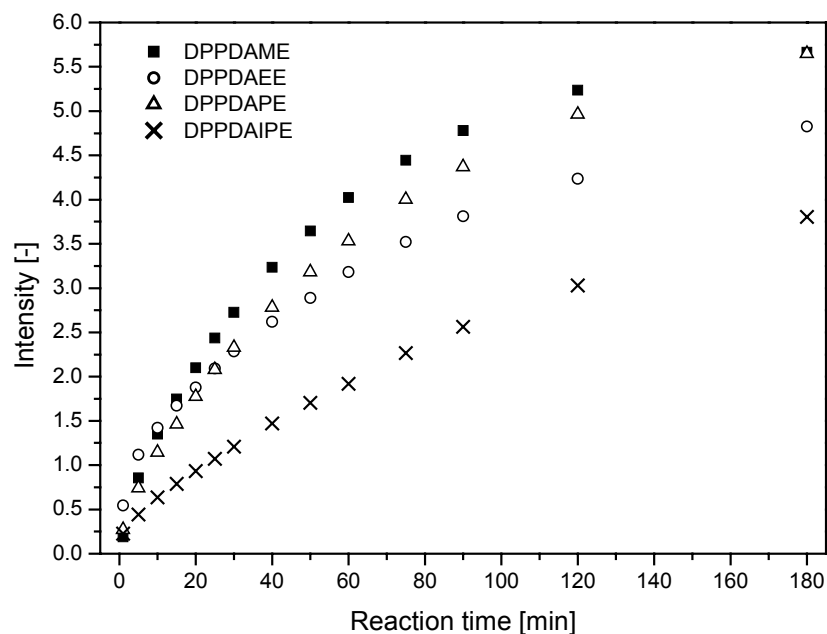


Figure 5.4: Time traces of the Eu(III) (10^{-3} mol/L) catalyzed hydrolysis of the DPPDA esters (10^{-5} mol/L)

Furthermore, the Eu(III) concentration was reduced. It was found out that an equimolar amount of Eu(III) is not sufficient to catalyze the ester cleavage with a satisfactory velocity. This could be explained by the assumption that the already formed acid molecules complex Eu(III) ions immediately. Therefore, the concentration of free uncomplexed Eu(III) which catalyzes the ester cleavage is reduced and the reaction velocity is significantly decreased.

The effect of temperature on the catalyzed ester cleavage was studied as well. The results are shown in figure 5.5, which contains the starting slopes of the temperature dependent time traces of the various ester cleavages.

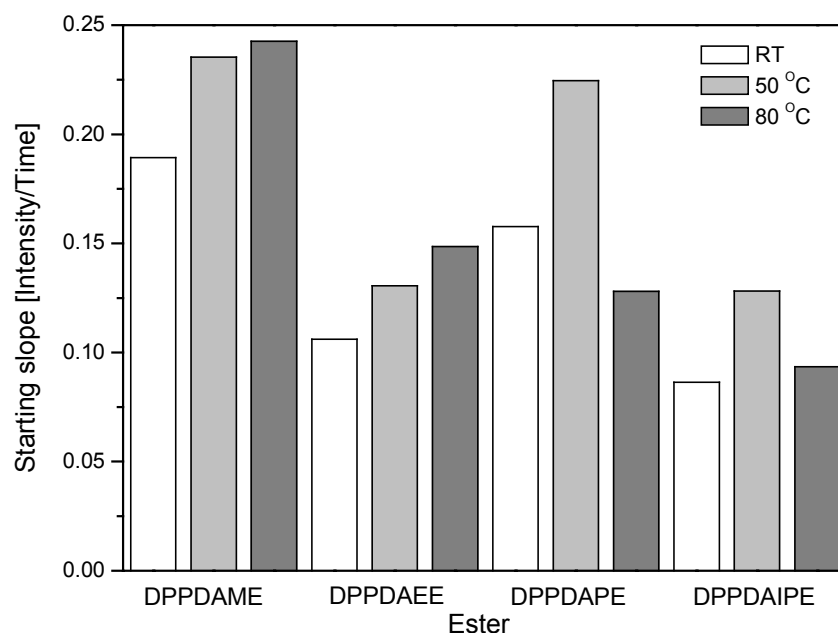


Figure 5.5: Temperature influence on the starting slopes of the time traces of the ester cleavage

In average, only a small increase of the catalytic activity was observed in the presence of Eu(III) when using elevated temperatures of 50 °C or 80 °C,

while the relative increase of the ester conversion in the absence of Eu(III) (blank experiment) was significantly higher. A possible explanation is a reduced complexation of the Eu(III) at the ester (see above), which leads to reduced catalytic activity and thus competes with the generally increasing reactivity at higher temperatures. Due to the limited benefits of a temperature variation, all further measurements in this work were carried out at room temperature.

It is important to find out, whether the DPPDA esters are the only alkyl esters which can be cleaved by Eu(III) ions. In order to employ a ligand comparable to DPPDA and which also exhibits lanthanide luminescence we chose 1,10-phenanthroline-2,9-dicarboxylic acid (PDA), which is a literature known sensitizer for Eu(III).[9] Therefore, the performed measurements could be directly compared. Figure 5.6 shows the reaction scheme of the PDA ester synthesis with subsequent ester cleavage by and complexation to Eu(III). This way only the dipropyl ester of PDA was synthesized.

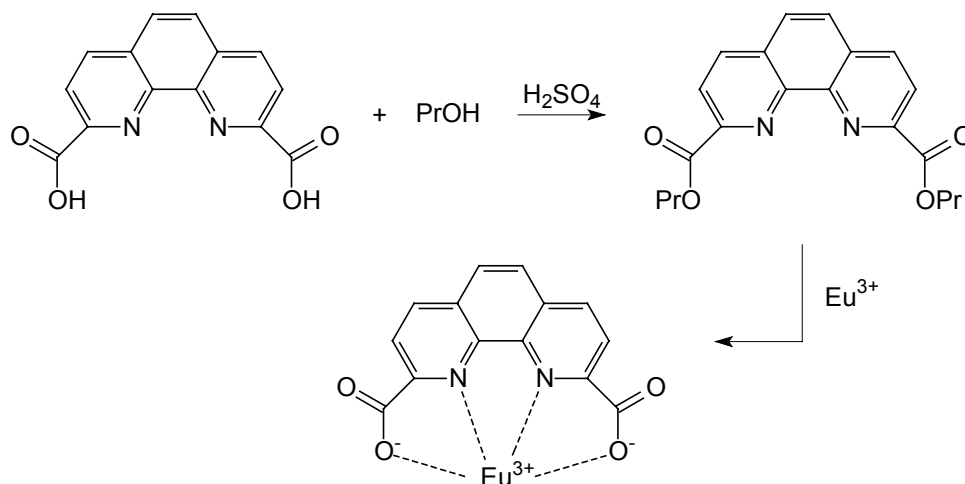


Figure 5.6: Reaction scheme of the PDA dipropyl ester synthesis with subsequent ester cleavage and complexation

In figure 5.7, the fluorescence spectra of the Eu(III)/PDA complex are presented. It is obvious that the excitation maximum is located at 290 nm, whereas the emission maximum expectedly is identical to that of DPPDA, which is due to the energy transfer to the Eu(III) ion.

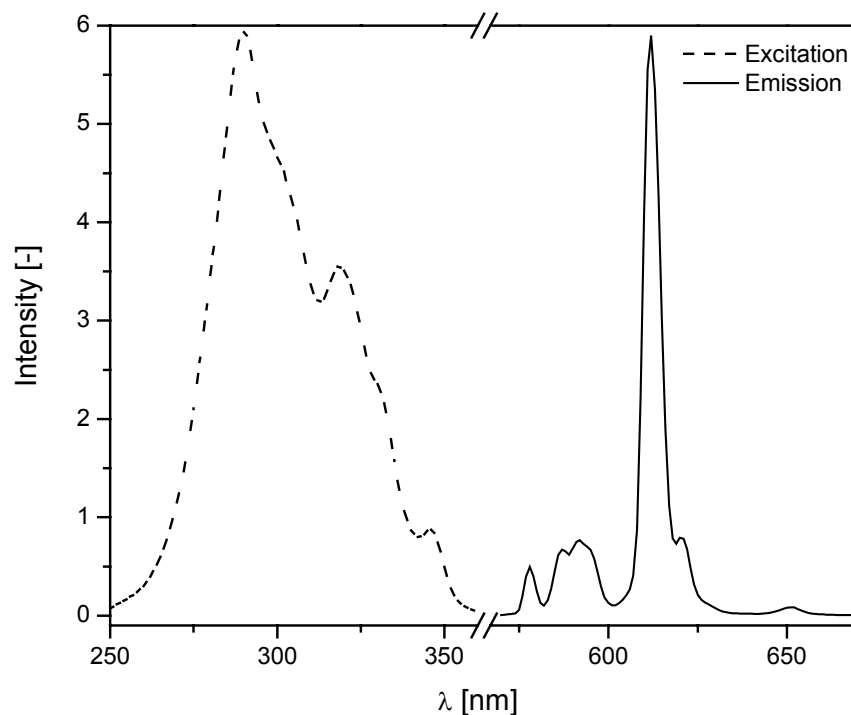


Figure 5.7: Fluorescence spectra of the Eu(III)/PDA complex

The time trace of the Eu(III) catalyzed cleavage of the PDA dipropyl ester was also recorded and the starting slope was determined. It was found out that the reaction is even slower than the conversion of the diisopropyl ester of DPPDA.

Further investigations should be performed concerning the catalytic activity of the other lanthanide(III) ions and related ions. As none of the other lanthanides is suitable to accept energy from DPPDA or PDA, it was not

possible to investigate the catalytic properties of the other lanthanides using lanthanide luminescence. Due to the fact that the free diacids of DPPDA and PDA are strong complexing agents and that they exhibit very similar UV/vis spectra, reversed-phase HPLC or UV/vis detection could not be applied to quantify the enzymatic conversion. However, it was possible to monitor the consumption of the diester and, with lower intensities due to an inferior ionization yield, the formation and subsequent consumption of the monoester by means of electrospray mass spectrometry (ESI-MS). Figure 5.8 shows a mass spectrum of the dimethyl ester of DPPDA. Inserted is the spectrum of the monomethyl ester.

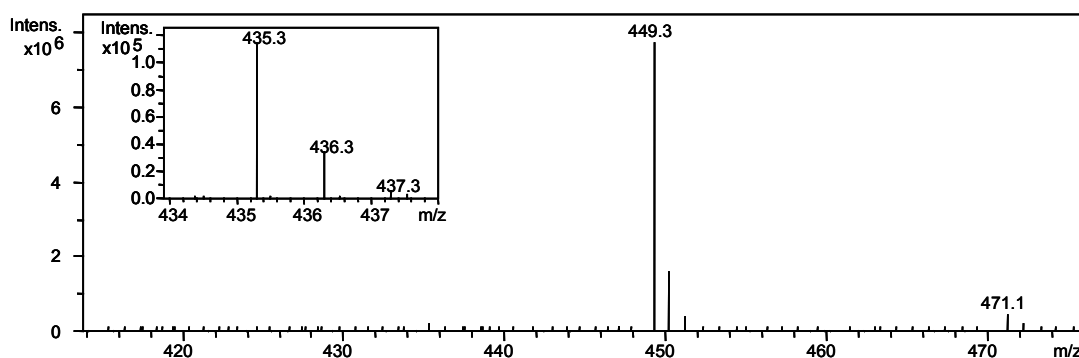


Figure 5.8: Mass spectrum of the dimethyl ester of DPPDA (10^{-5} mol/L); inserted is the extracted ion trace of the monomethyl ester of DPPDA

The reaction was carried out in an autosampler vial, and the mixture was injected into the mass spectrometer without separation. The respective results for the dimethyl ester of DPPDA with Eu(III) are presented in figure 5.9, with the signal of the monoester being enlarged by a factor of 100. During this time

period, no significant reduction of the concentration of the DPPDA dimethyl ester in the absence of Eu(III) was observed.

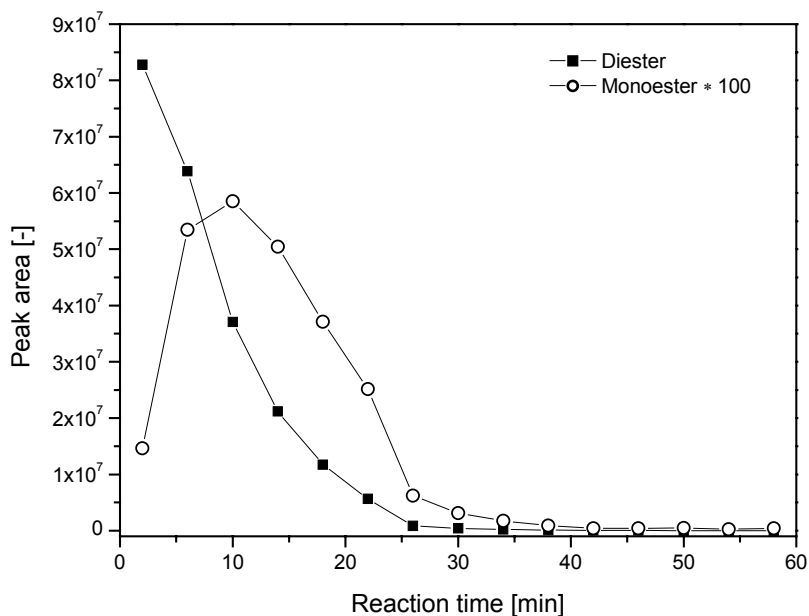


Figure 5.9: Consumption of the DPPDA dimethylester and the formation and subsequent consumption of the DPPDA monomethyl ester (enlarged by factor 100)

It is obvious that after a reaction time of 26 minutes, only 1% and after 54 minutes, only 0.01% of the initial concentration of the DPPDA dimethyl ester is observed. Therefore, an almost quantitative reaction is observed at room temperature within less than one hour. This indicates that the method might have the potential to be used in organic synthesis.

The complete series of lanthanide(III) cations plus Al(III), Fe(III), and Y(III) was then tested by ESI-MS with respect to their catalytic activities. As can be seen in figure 5.10, all lanthanides catalyze the ester cleavage, with the

greatest effect being observed for Sm(III), Eu(III) and Nd(III). La(III) and Fe(III) are characterized by low activities, while that of Al(III) is not significantly different from the blank. It was assumed that the different radii of the ions, which influence the complexation in a considerable way, might explain the observed tendencies. The radii are inserted in figure 5.10 and it becomes obvious that this is not the case. This fact will be subject to future investigations.

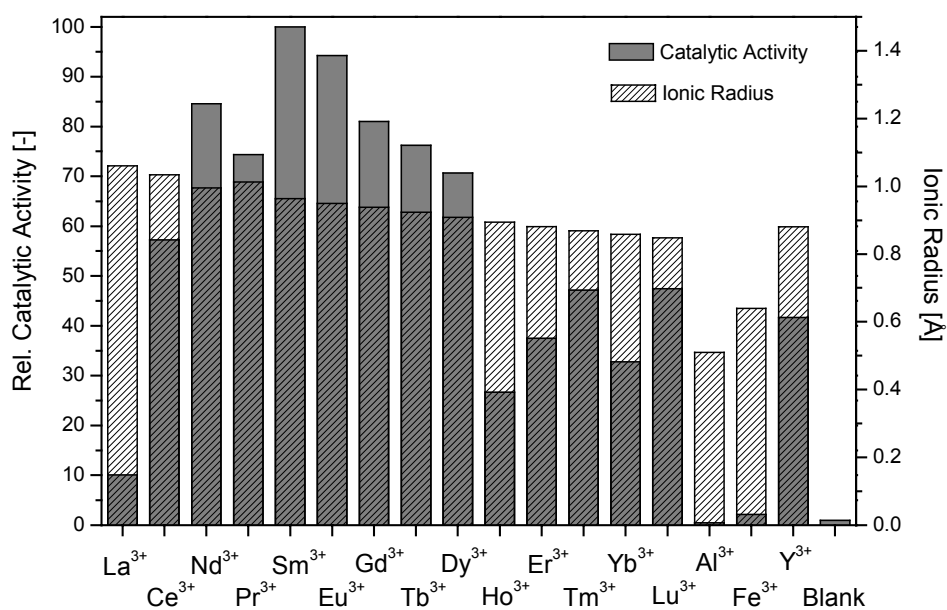


Figure 5.10: Catalytic activities of the lanthanide(III) ions, Al(III), Fe(III) and Y(III) towards the DPPDA dimethyl ester and ionic radii of the respective ions

It is known from literature that Eu(III) can catalyze the methanolysis of p-nitrophenyl esters.[7] Therefore, some investigations were performed on the methanolysis of the DPPDA dipropyl ester. As a rapid reaction was observed,

the concentration of Eu(III) was lowered to $2 \cdot 10^{-5}$ mol/L. The results can be seen in figure 5.11:

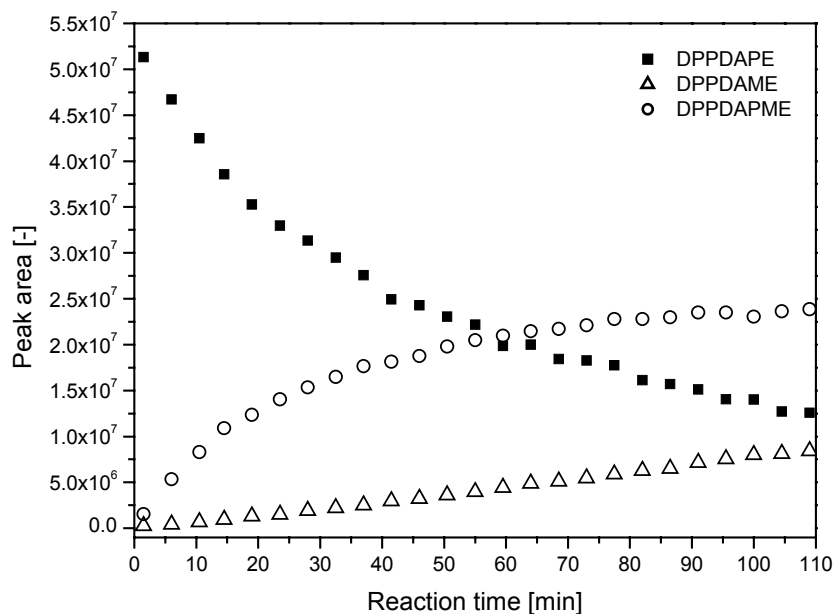


Figure 5.11: Time traces of the Eu(III) catalyzed methanolysis of the DPPDA dipropyl ester

It is obvious from the plot of the time traces that the signal of the DPPDA dipropyl ester decreases with time, whereas the signal of the DPPDA dimethyl ester and of the mixed DPPDA methyl propyl ester (DPPDAPME) increases and it can be deduced that Eu(III) catalyzes the methanolysis of the DPPDA dipropyl ester in a very effective way.

5.5 Conclusions

It can be concluded that the presented method is potentially useful for the hydrolysis of alkyl esters in aqueous/organic and, in the future possibly also in purely aqueous solutions. Further research on other groups of esters will

show if it is feasible to use this technique on a broader scale for the synthesis of carboxylic acids from the respective esters. A detailed investigation on the need for additional complexing groups would allow to deduce structure/functionality relationships with the goal to provide a preview, which esters might be cleaved by this catalytic method.

5.6 References

- [1] Evangelista, R. A.; Pollak, A.; Allore, B.; Templeton, E. F.; Morton, R. C.; Diamandis, E. P. *Clin. Biochem.* **1988**, 21, 173-178
- [2] Morton R. C.; Diamandis, E. P. *Anal. Chem.* **1990**, 62, 1841-1845
- [3] Chan, A.; Diamandis, E. P.; Kraijden, M.; *Anal. Chem.* **1993**, 65, 158-163
- [4] Scorilas, A.; Diamandis, E. P. *Clin. Biochem.* **2000**, 33, 345-350
- [5] Schneider, H.-J.; Rammo, J.; Hettich, R. *Angew. Chem. Int. Ed. Engl.* **1993**, 32, 1716-1719
- [6] Komiyama, M.; Takeda, N.; Shigekawa, H. *Chem. Commun.* **1999**, 16, 1443-1451
- [7] Neverov, A. A.; Gibson, G.; Brown, R. S. *Inorg. Chem.* **2003**, 42, 228-234
- [8] Neverov, A. A.; Monyoya-Pelaez, P. J.; Brown, R. S. *J. Am. Chem. Soc.* **2001**, 123, 210-217
- [9] Evangelista, R. A.; Pollak, A.; Gudgin Templeton, E. F. *Anal. Biochem.* **1991**, 197, 213-224
- [10] Takarada, T.; Takahashi, R.; Yashiro, M.; Komiyama, M. *J. Phys. Org. Chem.* **1998**, 11, 41-46

Concluding Remarks and Future Perspectives

Two different approaches to expand the applicability of enzyme-amplified lanthanide luminescence as detection method for bioassays have been presented within this thesis. Furthermore, it was shown that lanthanide(III) ions have the potential to catalyze the cleavage of certain alkyl esters in a very efficient way.

Chapter 3 describes the monitoring of an enzymatic reaction by means of EALL in comparison to the monitoring by ESI-MS. The results of both methods when following the ester cleavage of HL₁ showed good agreement and it can be concluded that they are useful when employing this type of substrates. The advantages of the EALL technique, are its simplicity and robustness, and in the possibility that it may already be carried out on a common, cheap standard fluorescence spectrometer. However, the reaction monitoring by means of ESI-MS is superior to the EALL method in some ways: When employing ESI-MS it is possible to determine not only the product increase, as it is the case with EALL, but also the substrate decrease. Furthermore, the ESI-MS method is, due to its high selectivity, likely to exhibit less interferences in complex matrices. However, both techniques should be considered as complementary techniques for the reaction monitoring of enzymatic conversions.

Chapter 4 describes a new EALL system for the determination of esterases and xanthine oxidase by means of Tb(III) or Eu(III) luminescence. In contrast to most of the other known EALL methods, it may be carried out at physiological pH, so that an addition of EDTA can be avoided, resulting in an even more simple detection scheme than the common EALL systems. In the future it may also be possible to use this EALL method for the determination of proteases, another interesting group of enzymes.

Chapter 5 describes the unexpected catalytic activity of lanthanide(III) ions towards the hydrolysis of 1,10-phenanthroline-2,9-dicarboxylic acid alkyl esters. Due to the high reaction velocity, simplicity and effectiveness of the catalysis by means of lanthanide(III) ions, this method may become useful for future applications. However, more research concerning other groups of esters for this reaction will have to be performed. A detailed investigation on the need for additional complexing groups for example, would allow to deduce structure/functionality relationships with the goal to provide a preview, which esters might be cleaved by this catalytic method.

Summary

Strategies to expand the range of applicability of the EALL detection scheme are presented within this thesis. First, it is described how the EALL method can be employed for the on-line monitoring of enzymatic conversions. The development of a new EALL system for the determination of one hydrolytic and one redox enzyme is presented, and the catalytic properties of lanthanide(III) ions towards the ester cleavage of certain model compounds are investigated.

The applicability of the EALL detection scheme for the monitoring of the esterase-catalyzed cleavage of the ethyl ester of bis(2-pyridylmethyl)-(2-acetoxyphenyl)amine was studied. The results were compared to those obtained with an independent method, namely ESI-MS. With the luminescence measurements, it was possible to record the product increase, whereas the ESI-MS measurements followed the product increase as well as the substrate decrease. The measurements for both methods were performed simultaneously and the results of both techniques were comparable.

A new EALL method for the determination of the enzymes esterase and xanthine oxidase has been developed. It employs 2,6-pyridinedicarboxylic acid (PDC) in combination with either Tb(III) or Eu(III). For the determination of the esterases, various esters of PDC have been synthesized, whereas for the determination of xanthine oxidase, 2,6-pyridinedicarboxaldehyde was

used. The methods for both enzymes were optimized with respect to pH, additives and time parameters and the time traces for all substrates have been recorded. It was found out that a nearly neutral pH is optimal for this EALL system and therefore the addition of EDTA could be avoided.

Studies on the catalytic activity of lanthanide(III) ions and other triply charged ions towards the ester cleavage of selected dialkyl esters have been performed. It was found out that the esters of 4,7-diphenyl-1,10-phenanthroline-2,9-dicarboxylic acid (DPPDA) and its derivatives are rapidly cleaved in the presence of lanthanide(III) ions. This phenomenon was further investigated with respect to its temperature dependency and the catalytic properties of the ions towards the methanolysis of one selected ester. All respective investigations were carried out by means of lanthanide luminescence and ESI-MS.

Samenvatting

In deze scriptie worden strategieën ter uitbreiding van het toepasbaarheidsbereik van de EALL detectietechniek gepresenteerd. Ten eerste wordt beschreven hoe de EALL methode kan worden gebruikt voor de on-line observatie van enzymatische omzettingen. De ontwikkeling van een nieuw EALL systeem voor de bepaling van een hydrolytisch en een redox enzym wordt voorgesteld en de katalytische eigenschappen van lanthanide(III) ionen met betrekking tot de ester klieving van bepaalde modelverbindingen zijn onderzocht.

De toepasbaarheid van de EALL detectiemethode voor het observeren van de door esterase gekatalyseerde klieving van de ethylester van bis(2-pyridythyl)-(2-acetoxyfenyl)amine is bestudeerd. De resultaten zijn vergeleken met die van een onafhankelijke methode, namelijk ESI-MS. Met de luminescentiemetingen was het mogelijk de toename van het reactieproduct te registreren, terwijl de ESI-MS metingen zowel de toename aan product als de afname aan substraat volgden. De metingen met beide methodes zijn simultaan uitgevoerd en de resultaten van beide technieken zijn vergelijkbaar.

Een nieuwe EALL methode is ontwikkeld voor de bepaling van de enzymen esterase en xanthine oxidase. Deze methode maakt gebruik van 2,6-pyridinedicarboxylzuur (PDC) in combinatie met Tb(III) of Eu(III). Voor de bepaling van de esterases zijn verschillende esters van PDC gesynthetiseerd,

waarbij voor de bepaling van xanthine oxidase 2,6-pyridinedicarboxaldehyde is gebruikt. De methodes voor beide enzymen zijn geoptimaliseerd wat betreft pH, additieven en tijdsparameters en voor alle substraten zijn de tijdcurves opgenomen. Een bijna neutrale pH is optimaal gebleken voor dit EALL systeem, waardoor de toevoeging van EDTA vermeden kon worden.

De katalytische activiteit van lanthanide(III)ionen en andere drievoudig geladen ionen met betrekking tot de ester klieving van een selectie dialkylesters is bestudeerd. Het is gebleken dat de esters van 4,7-difenyl-1,10-fenantroline-2,9-dicarboxylzuur (DPPDA) en zijn derivaten vlot gekliefd worden in de aanwezigheid van lanthanide(III) ionen. Dit fenomeen is verder onderzocht met betrekking tot de temperatuurafhankelijkheid en de katalytische eigenschappen van de ionen ten opzichte van de methanolyse van een bepaalde ester. Alle respectievelijke onderzoeken zijn uitgevoerd met behulp van lanthanide luminescentie en ESI-MS.

Acknowledgement

At the end of my thesis I like to thank all the people without who this work would never have been accomplished. Due to the fact that my Dutch is still rather poor, and therefore I can't thank you all in your native language, I decided to do this in one language and I chose one you all understand.

First, I thank Prof. Dr. Uwe Karst for the interesting research topic, the possibility to attend international conferences, even abroad and for his overall support. The time he spends and the interest he shows towards the research of his coworkers cannot be taken for granted.

Then there are to be mentioned all my colleague PhD students: Georg Diehl, Sebastian Götz, Heiko Hayen whom I thank especially for the work at the MS he did for me, Christel Hempen, my favorite roommate who gave me more than only scientific support, Hartmut Henneken, Nicole Jachmann (I still owe you for the bike!), André Liesener, with whom I worked together for the reaction monitoring, Jörg Meyer, Tobias Revermann, Rasmus Schulte-Ladbeck, Bettina Seiwert, Suze van Leeuwen, who translated the summary of this thesis into dutch, and Martin Vogel (our 'Mini-Boss'), whom I thank especially for all the paper work he accomplished for me. I would like to thank you all for the nice and relaxed working atmosphere in our labs and I will also never forget all those happy discussions we had about (sometimes extremely) non-scientific things in our breaks and spare time.

Acknowledgement

Furthermore, I want to thank our technical staff and our two secretaries: Nancy Heijnekamp-Snellens, for organizing things and ordering everything even on short notice, Martijn Heuven, Annemarie Montanaro-Christenhusz, especially for performing the elemental analysis measurements, Saskia Tekkelenburg-Rompelman and Susanne van Rijn. The openness and the uncomplicated manner with which you all welcomed us, cannot be taken for granted. I also want to thank you all for the nice working atmosphere and the insights in the Dutch way of life you offered to us in the last two and a half years.

I also don't want to forget to thank the Group of Prof. Andersson back in Münster, and especially Benedikte Roberz, for their support even after we left for the Netherlands.

Last but not least I would like to thank my family, Indra and Sebastian for all the non-analytical support I received from them.

Curriculum Vitae

PERSONAL DETAILS

- **Name:** Tanja Steinkamp
- **Nationality:** German
- **Date of Birth:** 10.03.1976
- **Born in:** Ankum, Germany

EDUCATION

- **1982 - 1986** Elementary School in Rieste, Germany
- **1986 – 1988** Orientierungsstufe Bersenbrueck, Bersenbrück, Germany
- **1988 - 1995** Gymnasium Bersenbrück, Bersenbrück, Germany
- **1995 – 2000** Studies of Chemistry at the University of Münster, Germany
Intermediate exam in October 1998
Graduation (diploma) in December 2000
thesis: “*A New System of Ligands for Enzyme Amplified Time Resolved Fluorescence Spectroscopy Using Lanthanide Complexes*”
- **01/2001** Begin of the dissertation in Analytical Chemistry at the University Münster (Germany) with Prof. Dr. U. Karst
- **10/2001** Continuation of the dissertation at the University of Twente (Enschede, The Netherlands) with Prof. Dr. U. Karst

List of Publications

Original Papers

1. A tripod ligand as new sensitizer for the enzyme amplified lanthanide luminescence determination of esterase
Steinkamp, T.; Schweppe, F.; Krebs, B.; Karst, U. *Analyst* **2003**, 128, 29-31
2. Reaction Monitoring of Enzyme-catalyzed Ester Cleavage by Time Resolved Fluorescence and Electrospray Mass Spectrometry: Method Development and Comparison
Steinkamp, T.; Liesener, A.; Karst, U. *Anal. Bioanal. Chem.* **2004**, 378, 124-1128
3. Detection Scheme for Bioassays Based on 2,6-Pyridinedicarboxylic Acid Derivatives and Enzyme-Amplified Lanthanide Luminescence
Steinkamp, T.; Karst, U. *Anal. Chem.*, submitted for publication
4. Lanthanide-catalyzed hydrolysis of 4,7-diphenyl-1,10-phenanthroline-2,9-dicarboxylic acid esters
Steinkamp, T.; Hayen, H.; Karst, U. *Chem. Comm.*, submitted for publication
5. Detection Strategies for Bioassays Based on Luminescent Lanthanide Complexes and Signal Amplification
Steinkamp, T.; Karst, U. *Anal. Bioanal. Chem.*, accepted for publication

Other Paper

1. Liesener, A.; Steinkamp, T.; Karst, U. *GIT Laborfachzeitschrift* **2004**, 5, 454-457
Massenspektrometrische Detektion in Bioassays – Herausforderungen und Chancen

Patent

1. Steinkamp, T.; Schweppe, F.; Krebs, B.; Karst, U.
Verfahren zur Bestimmung hydrolytischer Enzyme
Patent No. DE10102839, Publication Date 2002, August 01.

Oral Presentations

1. Tanja Steinkamp, Jörg Meyer and Uwe Karst
New Applications for the Enzyme Amplified Lanthanide Luminescence
Pittcon 2001, March 4.-9. (New Orleans, Louisiana, USA)
2. Tanja Steinkamp, Jörg Meyer and Uwe Karst
Enzymverstärkte zeitverzögerte Fluoreszenz von Lanthanoidchelaten
als Detektionsverfahren in der Bioanalytik
Incom 2001, March 27.-29. (Düsseldorf, Germany)
3. Tanja Steinkamp and Uwe Karst
New Groups of Ligands for Enzyme-Amplified Lanthanide
Luminescence
Pittcon 2002, March 17.-22. (New Orleans, Louisiana, USA)

4. Tanja Steinkamp, André Liesener and Uwe Karst
Enzyme Amplified Lanthanide Luminescence for the Determination of
Enzyme Labels
Pittcon 2003, March 9.-14. (Orlando, Florida, USA)
5. Tanja Steinkamp and Uwe Karst
Lanthanoidchelate zur hochselektiven Detektion in der Bioanalytik
Incom 2003, March 25.-27. (Düsseldorf, Germany)

